

# Chapter 3

## Non-ideal Gases

This chapter is devoted to considering systems where the interactions between particles can no longer be ignored. We note that in the previous chapter we did indeed consider, albeit briefly, the effects of interactions in fermion and in boson gases. This chapter is concerned more with a systematic treatment of interatomic interactions. Here the quantum aspect is but a complication and most of the discussions will thus take place within the context of a classical description.

### 3.1 Statistical Mechanics of Interacting Particles

#### 3.1.1 The partition function

We are now considering gases where the interactions between the particles cannot be ignored. Our starting point is that everything can be found from the partition function. We will work, initially, in the classical framework where the energy function of the system is

$$H(p_i, q_i) = \sum_i \frac{p_i^2}{2m} + \sum_{i < j} U(q_i, q_j). \quad (3.1.1)$$

Because of the interaction term  $U(q_i, q_j)$  the partition function can no longer be factorised into the product of single-particle partition functions. The many-body partition function is

$$Z = \frac{1}{N! h^{3N}} \int e^{-(\sum_i p_i^2/2m + \sum_{i < j} U(q_i, q_j))/kT} d^{3N}p d^{3N}q \quad (3.1.2)$$

where the factor  $1/N!$  is used to account for the particles being indistinguishable.

While the partition function cannot be factorised into the product of single-particle partition functions, we can factor out the partition function for the non-interacting case since the energy is a sum of a momentum-dependent term (kinetic energy) and a coordinate-dependent term (potential energy). The non-interacting partition function is

$$Z_{\text{id}} = \frac{V^N}{N!h^{3N}} \int e^{-(\sum_i p_i^2/2m)/kT} d^{3N}p \quad (3.1.3)$$

where the  $V$  factor comes from the integration over the  $q_i$ . Thus the interacting partition function is

$$Z = Z_{\text{id}} \frac{1}{V^N} \int e^{-(\sum_{i<j} U(q_i, q_j))/kT} d^{3N}q. \quad (3.1.4)$$

The “correction term” is referred to as the configuration integral. We denote this by  $Q$

$$Q = \frac{1}{V^N} \int e^{-(\sum_{i<j} U(q_i, q_j))/kT} d^{3N}q. \quad (3.1.5)$$

(Different authors have different pre-factors such as  $V$  or  $N!$ , but that is not important.) The partition function for the interacting system is then

$$Z = \frac{1}{N!} \left( \frac{V}{\Lambda^3} \right)^N Q \quad (3.1.6)$$

and the attention now focuses on evaluation/approximation of the configuration integral  $Q$ .

### 3.1.2 Cluster expansion

We need a quantity in terms of which to perform an expansion. To this end we define

$$f_{ij} = e^{-U(q_i, q_j)/kT} - 1, \quad (3.1.7)$$

which has the property that  $f_{ij}$  is only appreciable when the particles are close together. In terms of this parameter the configuration integral is

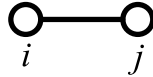
$$Q = \frac{1}{V^N} \int \prod_{i<j} (1 + f_{ij}) d^{3N}q_i \quad (3.1.8)$$

where the exponential of the sum has been factored into the product of exponentials.

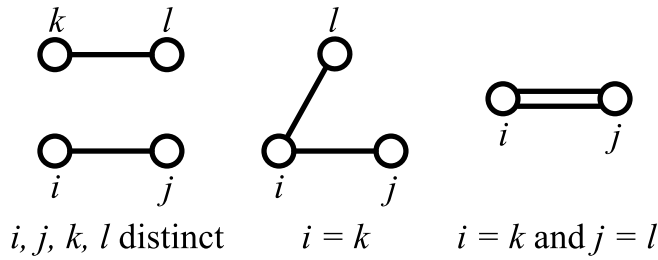
Next we expand the product as:

$$\prod_{i < j} (1 + f_{ij}) = 1 + \sum_{i < j} f_{ij} + \sum_{i < j} \sum_{k < l} f_{ij} f_{kl} + \dots \quad (3.1.9)$$

The contributions to the second term are significant whenever pairs of particles are close together. Diagrammatically we may represent the contributions to the second term as:



Contributions to the third term are significant either, if  $i, j, k, l$  are distinct, when pairs  $i - j$  and  $k - l$  are simultaneously close together or, if  $j = k$  in the sums, when triples  $i, j, l$  are close together. The contributions to the third term may be represented as:



The contributions to the higher order terms may be represented in a similar way. The general expansion in this way is called a “cluster expansion” for obvious reasons.

### 3.1.3 Low density approximation

In the case of a dilute gas, we need only consider the effect of pairwise interactions – the first two terms of Eq. (3.1.9). This is because while the probability of two given particles being simultaneously close is small, the probability of three atoms being close is vanishingly small. Then we have

$$\prod_{i < j} (1 + f_{ij}) \approx 1 + \sum_{i < j} f_{ij} \quad (3.1.10)$$

so that, within this approximation,

$$\begin{aligned} Q &= \frac{1}{V^N} \int \left\{ 1 + \sum_{i < j} f_{ij} \right\} d^{3N} q_i \\ &= 1 + \int \sum_{i < j} f_{ij} d^{3N} q_i. \end{aligned} \quad (3.1.11)$$

There are  $N(N-1)/2$  terms in the sum since we take all pairs without regard to order. And for large  $N$  this may be approximated by  $N^2/2$ . Since the particles are identical, each integral in the sum will be the same, so that

$$Q = 1 + \frac{N^2}{2V} \int f_{12} d^3r_{12}. \quad (3.1.12)$$

The  $V^N$  in the denominator has now become  $V$  since the integration over  $i, j \neq 1, 2$  gives a factor  $V^{N-1}$  in the numerator.

Finally, then, we have the partition function for the interacting gas:

$$Z = Z_{\text{id}} \left\{ 1 + \frac{N^2}{2V} \int [e^{-U(\mathbf{r})/kT} - 1] d^3r \right\} \quad (3.1.13)$$

and on taking the logarithm, the free energy is the sum of the non-interacting gas free energy and the new term

$$F = F_{\text{id}} - kT \ln \left\{ 1 + \frac{N^2}{2V} \int [e^{-U(\mathbf{r})/kT} - 1] d^3r \right\}. \quad (3.1.14)$$

Since  $U(r)$  may be assumed to be spherically symmetric, in spherical polars we can integrate over the angular coordinates:

$$\int \dots d^3r \rightarrow 4\pi \int r^2 \dots dr \quad (3.1.15)$$

to give

$$F = F_{\text{id}} - kT \ln \left\{ 1 + \frac{N^2}{2V} 4\pi \int r^2 [e^{-U(r)/kT} - 1] dr \right\}. \quad (3.1.16)$$

In this low density approximation the second term in the logarithm, which accounts for pairwise interactions, is much less than the first term. — Otherwise the third and higher-order terms would also be important. But if the second term is small then the logarithm can be expanded. Thus we obtain

$$F = F_{\text{id}} - 2\pi kT \frac{N^2}{V} \int r^2 [e^{-U(r)/kT} - 1] dr. \quad (3.1.17)$$

A more rigorous treatment of the cluster expansion technique, including the systematic incorporation of the higher-order terms, is given in the article by Mullin [1].

### 3.1.4 Equation of state

The pressure is found by differentiating the free energy:

$$\begin{aligned} p &= - \left. \frac{\partial F}{\partial V} \right|_{T,N} \\ &= kT \frac{N}{V} - kT \frac{N^2}{V^2} 2\pi \int r^2 [e^{-U(r)/kT} - 1] dr. \end{aligned} \quad (3.1.18)$$

We see that the effect of the interaction  $U(r)$  can be regarded as modifying the pressure from the ideal gas value. The net effect can be either attractive or repulsive; decreasing or increasing the pressure. This will be examined, for various model interaction potentials  $U(r)$ . However before that we considered a systematic way of generalising the gas equation of state.

## 3.2 The Virial Expansion

### 3.2.1 Virial coefficients

At low densities we know that the equation of state reduces to the ideal gas equation. A systematic procedure for generalising the equation of state would therefore be as a power series in the number density  $N/V$ . Thus we write

$$\frac{p}{kT} = \frac{N}{V} + B_2(T) \left(\frac{N}{V}\right)^2 + B_3(T) \left(\frac{N}{V}\right)^3 + \dots \quad (3.2.1)$$

The  $B$  factors are called *virial coefficients*;  $B_n$  is the  $n^{\text{th}}$  virial coefficient. By inspecting the equation of state derived above, Eq. (3.1.18), we see that it is equivalent to an expansion up to the second virial coefficient. And the second virial coefficient is given by

$$B_2(T) = -2\pi \int_0^\infty r^2 [e^{-U(r)/kT} - 1] dr \quad (3.2.2)$$

which should be “relatively” easy to evaluate once the form of the interparticle interaction  $U(r)$  is known. It is also possible to calculate higher order virial coefficients, but it becomes more difficult.

### 3.2.2 Hard core potential

(The reader is referred to Reichl [2] for further details some of the models in the following sections.)

The hard core potential is specified by

$$\begin{aligned} U(r) &= \infty & r < \sigma \\ &= 0 & r > \sigma. \end{aligned} \quad (3.2.3)$$

Here the single parameter  $\sigma$  is the hard core diameter: the closest distance between the centres of two particles. This is modelling the particles as impenetrable spheres. There is no interaction when the particles are separated greater than  $\sigma$  and they are prevented, by the interaction, from getting any closer than  $\sigma$ . It should, however, be noted that this model interaction is un-physical since it only considers the repulsive part; there is no attraction at any separation.

The gas of hard sphere particles is considered in some detail in Section 3.6. For the present we are concerned solely with the second virial coefficient.

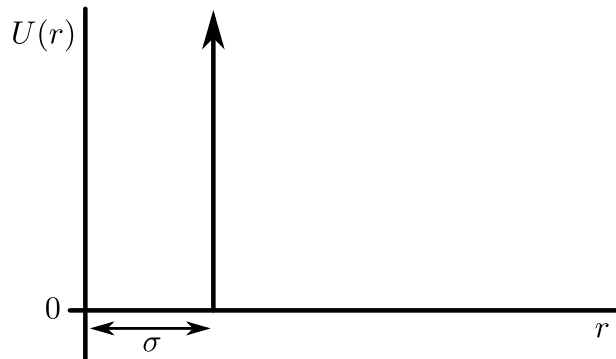


Figure 3.1: Hard core potential

For this potential we have

$$\begin{aligned} e^{-U(r)/kT} &= 0 & r < \sigma \\ &= 1 & r > \sigma \end{aligned} \quad (3.2.4)$$

so that the expression for  $B_2(T)$  is

$$\begin{aligned} B_2(T) &= 2\pi \int_0^\sigma r^2 dr \\ &= \frac{2}{3}\pi\sigma^3. \end{aligned} \quad (3.2.5)$$

In this case we see that the second virial coefficient is independent of temperature, and it is always positive. The (low density) equation of state is then

$$pV = NkT \left\{ 1 + \frac{2}{3}\pi\sigma^3 \frac{N}{V} \right\} \quad (3.2.6)$$

which indicates that the effect of the hard core is to increase the  $pV$  product over the ideal gas value.

It is instructive to rearrange this equation of state. We write it as

$$pV \left\{ 1 + \frac{2}{3}\pi\sigma^3 \frac{N}{V} \right\}^{-1} = NkT \quad (3.2.7)$$

and we note that the “correction” term  $\frac{2}{3}\pi\sigma^3 N/V$  is small within the validity of the derivation; it is essentially the hard core volume of a particle divided by the total volume per particle. So performing a binomial expansion we find to the same leading power of density

$$pV \left\{ 1 - \frac{2}{3}\pi\sigma^3 \frac{N}{V} \right\} = NkT \quad (3.2.8)$$

or

$$p \left\{ V - \frac{2}{3}N\pi\sigma^3 \right\} = NkT. \quad (3.2.9)$$

In this form we see that the effect of the hard core can be interpreted as simply reducing the available volume of the system.

### Excluded volume

By how much is the volume reduced? Two spheres of *diameter*  $\sigma$  cannot approach each other closer than this distance. As indicated in Fig. 3.2 this means that the effect of one particle is to exclude a sphere of *radius*  $\sigma$  from the other particle.

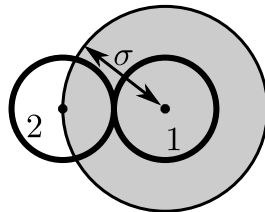


Figure 3.2: Volume of space excluded to particle 2 by particle 1

Two particles exclude a volume  $\frac{4}{3}\pi\sigma^3$ . Thus the “excluded volume” per particle is *one half* of this. And the excluded volume of  $N$  particles is then

$$V_{\text{ex}} = \frac{2}{3}N\pi\sigma^3, \quad (3.2.10)$$

that is, *four* times the volume of the particles. This is precisely the volume reduction of Eq. (3.2.9).

We should note that the second virial coefficient for the hard sphere gas is then simply the excluded volume per particle.

### 3.2.3 Square-well potential

The square-well potential is somewhat more realistic than the simple hard core potential; it includes a region of attraction as well as the repulsive hard core. The potential is specified by

$$\begin{aligned} U(r) &= \infty & r < \sigma \\ &= -\varepsilon & \sigma < r < R\sigma \\ &= 0 & R\sigma < r \end{aligned} \quad (3.2.11)$$

so we see that it depends on three parameters:  $\sigma$ ,  $\varepsilon$  and the dimensionless  $R$ .

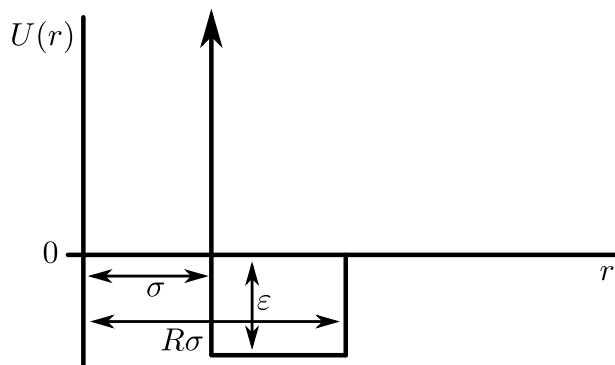


Figure 3.3: Square well potential

For this potential we have

$$\begin{aligned} e^{-U(r)/kT} &= 0 & r < \sigma \\ &= e^{\varepsilon/kT} & \sigma < r < R\sigma \\ &= 1 & R\sigma < r \end{aligned} \quad (3.2.12)$$



so that the expression for  $B_2(T)$  is

$$\begin{aligned} B_2(T) &= -2\pi \left\{ (-1) \int_0^\sigma r^2 dr + (e^{\varepsilon/kT} - 1) \int_\sigma^{R\sigma} r^2 dr \right\} \\ &= \frac{2}{3}\pi\sigma^3 \left\{ 1 - (R^3 - 1) (e^{\varepsilon/kT} - 1) \right\} \end{aligned} \quad (3.2.13)$$

or

$$\begin{aligned} B_2(T) &= \frac{2}{3}\pi\sigma^3 \left\{ R^3 - (R^3 - 1)e^{\varepsilon/kT} \right\} \\ &= \frac{2}{3}\pi\sigma^3 R^3 - \frac{2}{3}\pi\sigma^3 (R^3 - 1)e^{\varepsilon/kT}. \end{aligned} \quad (3.2.14)$$

In this case, using the more realistic potential, we see that the second virial coefficient depends on temperature, varying as

$$B_2(T) = A - Be^{\varepsilon/kT}. \quad (3.2.15)$$

The second virial coefficient for nitrogen is shown in Fig. 3.4. The square well curve of Eq. (3.2.14) has been fitted through the data with  $\varepsilon/k = 88.3 \text{ K}$ ,  $\sigma = 3.27 \text{ \AA}$  ( $1 \text{ \AA} = 10^{-10} \text{ m}$ ), and  $R = 1.62$ . Observe that this crude approximation to the inter-particle interaction gives a remarkably good agreement with the experimental data. The figure also shows the hard sphere asymptote  $B_2^{\text{hs}} = 44.28 \text{ cm}^3/\text{mol}$ .

At low temperatures, where  $B_2(T)$  is negative, this indicates that the attractive part of the potential is dominant and the pressure is reduced compared with the ideal gas case. And at higher temperatures, where it is intuitive that the small attractive part of the potential will have negligible effect,  $B_2(T)$  will be positive and the pressure will be increased, as in the hard sphere case. The temperature at which  $B_2(T)$  goes through zero is called the *Boyle temperature*, denoted by  $T_B$ . For the square well potential

$$T_B = \frac{-\varepsilon/k}{\ln\left(1 - \frac{1}{R^3}\right)} \quad (3.2.16)$$

At very high temperatures we see from the expression for  $B_2(T)$  that it saturates at the hard core excluded volume.

### 3.2.4 Lennard-Jones potential

The Lennard-Jones potential is a very realistic representation of the inter-atomic interaction. It comprises an attractive  $1/r^6$  term with a repulsive

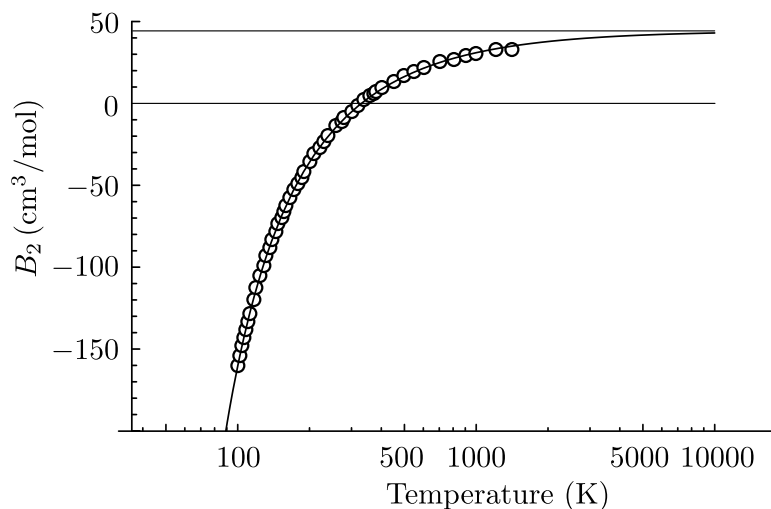


Figure 3.4: Second virial coefficient of nitrogen as a function of temperature with the square well functional form Eq. (3.2.14). Square well parameters  $\varepsilon/k = 88.3$  K,  $\sigma = 3.27$  Å, and  $R = 1.62$ .

$1/r^{12}$  term. The form of the attractive part is well-justified as a description of the attraction arising from fluctuating electric dipole moments. The repulsive term is simply a power law approximation to the effect of the overlap of the atoms' external electron clouds. We write the Lennard-Jones potential as

$$U(r) = 4\varepsilon \left\{ \left( \frac{\sigma}{r} \right)^{12} - \left( \frac{\sigma}{r} \right)^6 \right\}; \quad (3.2.17)$$

this depends on the two parameters:  $\varepsilon$  and  $\sigma$  as shown in Fig. 3.5.

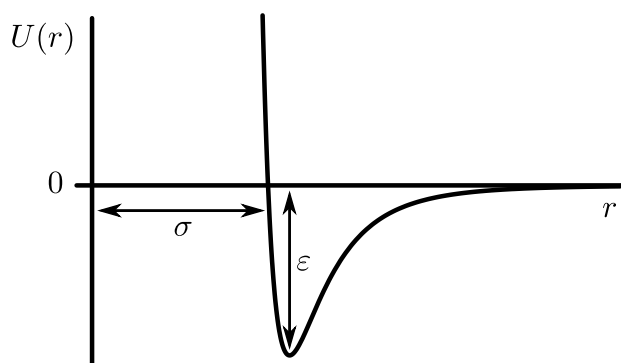


Figure 3.5: Lennard-Jones 6–12 potential

The integral for the second virial coefficient is

$$B_2(T) = -2\pi \int_0^\infty r^2 \left[ e^{-\frac{4\varepsilon}{kT} \left\{ \left(\frac{r}{\sigma}\right)^{12} - \left(\frac{r}{\sigma}\right)^6 \right\}} - 1 \right] dr. \quad (3.2.18)$$

By making the substitution  $x = r/\sigma$  we cast this as

$$B_2(T) = -2\pi\sigma^3 \int_0^\infty x^2 \left[ e^{-4(x^{12} - x^6)\varepsilon/kT} - 1 \right] dx. \quad (3.2.19)$$

This is instructive. The  $\sigma$ -dependence is all in the hard core pre-factor and the integral depends on temperature solely through the combination  $kT/\varepsilon$ .

It is possible to express the integral of Eq. (3.2.19) in terms of a Hermite function  $H_n(x)$ <sup>1</sup>. In this way we obtain:

$$B_2(T) = \frac{2}{3}\pi\sigma^3 \sqrt{2\pi} \left(\frac{\varepsilon}{kT}\right)^{1/4} H_{\frac{1}{2}} \left(-\sqrt{\frac{\varepsilon}{kT}}\right). \quad (3.2.20)$$

This is an elegant closed-form expression for the second virial coefficient of the Lennard-Jones gas.

This is plotted in Fig. 3.6 together with the data from nitrogen. The curve has been fitted with parameters  $\varepsilon/k = 95.5$  K,  $\sigma = 3.76$  Å. The figure also shows the “hard sphere” asymptote  $B_2^{\text{hs}} = 67.00$  cm<sup>3</sup>/mol. The fit is good. We see that the Lennard-Jones calculated form shows reduction in  $B_2$  at higher temperatures, where the energetic collisions can cause the atoms to come even closer together; the “hard core” is not so hard. This effect is observed in helium, shown in Fig. 3.11. We find, from (3.2.20), that the maximum value,  $B_2^{\text{max}} = 0.529 \times \frac{2}{3}\pi\sigma^3$  occurs at  $T = 25.13 \varepsilon/k$ .

From the zero of the Hermite function we find the Boyle temperature to be

$$T_B = 3.418\varepsilon/k. \quad (3.2.21)$$

At high temperatures we have the expansion<sup>2</sup>

$$\begin{aligned} B_2(T) = \frac{2}{3}\pi\sigma^3 \left\{ \frac{2\pi}{\Gamma(1/4)} \left(\frac{\varepsilon}{kT}\right)^{1/4} - \frac{\pi}{\Gamma(3/4)} \left(\frac{\varepsilon}{kT}\right)^{3/4} \right. \\ \left. - \frac{2\pi}{\Gamma(5/4)} \left(\frac{\varepsilon}{kT}\right)^{5/4} - \frac{\pi}{8\Gamma(7/4)} \left(\frac{\varepsilon}{kT}\right)^{7/4} - \frac{5\pi}{64\Gamma(9/4)} \left(\frac{\varepsilon}{kT}\right)^{9/4} + \dots \right\} \end{aligned} \quad (3.2.22)$$

<sup>1</sup>The Hermite polynomials  $H_n(x)$  should be familiar, from the quantum mechanics of the harmonic oscillator. For integer order  $n$ ,  $H_n(x)$  is a polynomial of power  $n$  in  $x$ . Hermite *functions* generalize to the case of non-integer order; such functions are no longer finite polynomials. We follow the *Mathematica* definition and terminology whereby the same symbol is used for both: `HermiteH[n, x]`.

<sup>2</sup>This series is obtained by a direct term-by-term expansion of the Hermite function.

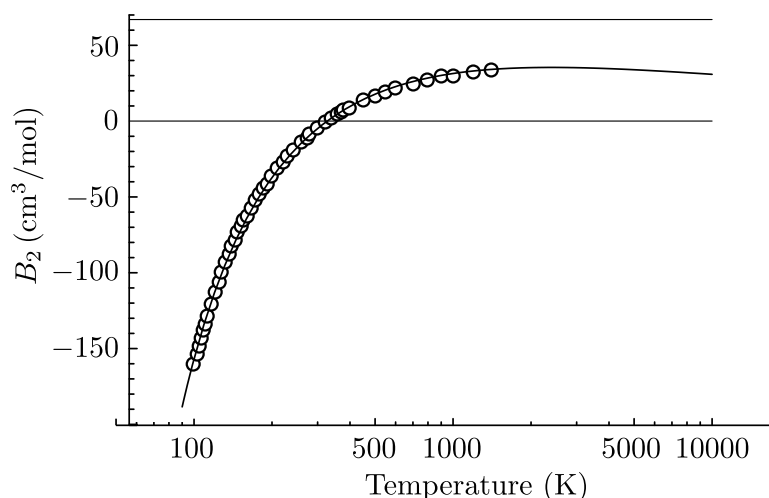


Figure 3.6: Second virial coefficient of nitrogen plotted with the Lennard-Jones functional form, Eq. (3.2.20). Lennard-Jones parameters  $\varepsilon/k = 95.5$  K,  $\sigma = 3.76$  Å.

or, in closed form<sup>3</sup>

$$B_2(T) = -\frac{2}{3}\pi\sigma^3 \sum_{n=0}^{\infty} \frac{1}{(4n)!} \Gamma\left(\frac{2n-1}{4}\right) \left(\frac{4\varepsilon}{kT}\right)^{(2n+1)/4}. \quad (3.2.23)$$

At low temperatures we have the expansion<sup>4</sup>

$$B_2(T) = -\frac{2}{3}\pi\sigma^3 \times e^{\varepsilon/kT} \times \sqrt{\frac{\pi}{2}} \left\{ \left(\frac{kT}{\varepsilon}\right)^{1/2} + \frac{15}{16} \left(\frac{kT}{\varepsilon}\right)^{3/2} + \frac{945}{512} \left(\frac{kT}{\varepsilon}\right)^{5/2} + \dots \right\}. \quad (3.2.24)$$

### A comment on scaling

The Lennard-Jones potential has two parameters: an energy  $\varepsilon$  and a length  $\sigma$ . We note that these happen to correspond to the vertical and the horizontal axes of the plot of  $U(r)$  against  $r$ . This means that the Lennard-Jones potential has the form of a *universal* function that just needs the appropriate scaling in the  $U$  and  $r$  directions. And by extension this tells us that for any system of particles which interact with a Lennard-Jones potential, those properties that depend on the inter-particle potential, similarly, will have a

<sup>3</sup>To obtain this expression Eq. (3.2.19) is integrated by parts, the exponential is then expanded and the integration performed term by term.

<sup>4</sup>This is quoted from a calculation by Gutierrez [3].

universal form when the energies are scaled by  $\varepsilon$ , the distances by  $\sigma$  and other variables in the corresponding way.

It follows that any inter-particle potential which has only two adjustable (system-specific) parameters with different dimensions, will possess this scaling property. A special case of this is the hard sphere interaction which has only one parameter; we may regard this as having an energy parameter of zero. But we recognize immediately that the square well potential, with *three* parameters  $\varepsilon$ ,  $\sigma$  and the dimensionless distance ratio  $R$  does *not* possess the scaling property. But if  $R$  were to be regarded as *fixed* then the two parameters  $\varepsilon$  and  $\sigma$  would lead to universal behaviour. Indeed for the inert gases neon, argon, krypton and xenon the values of  $R$  are close: approximately 1.65.

It is clear that two-parameter potentials, and their resultant universal system properties are particularly convenient in statistical mechanics. This is one of the reasons for the popularity of the Lennard-Jones function where the dipolar attraction and the electron shell repulsion – two very different phenomena – are parameterized in similar ways: both having energies scaling with the same  $\varepsilon$  and distances scaling with the same  $\sigma$ .

And in this vein the Sutherland potential of the next session and the “soft sphere” interaction treated in Problem 3.16 both possess the scaling property.

### 3.2.5 The Sutherland potential

The interaction between atoms or molecules comprises a repulsive part at short distances and an attractive part at large distances. The Lennard-Jones potential of the previous section is often used as an analytical representation of the interaction. As we explained, the attractive tail is well-described by the  $r^{-6}$  law, while the  $r^{-12}$  description of the repulsive core is but a simple approximation to the actual short-range interaction. The popularity of the 6–12 potential lies principally in its mathematical elegance.

The Sutherland potential treats the short-distance repulsion in a different way; it approximates the interaction as a hard core. The attractive tail is described by the conventional dipolar  $r^{-6}$  law.

The form of the Sutherland potential is shown in Fig. 3.7; it is specified by

$$\begin{aligned} U(r) &= \infty & r < \sigma \\ &= -\varepsilon \left(\frac{\sigma}{r}\right)^6 & r > \sigma. \end{aligned} \quad (3.2.25)$$

As with the Lennard-Jones potential, the Sutherland potential has a universal form, scaled vertically with an energy parameter  $\varepsilon$  and horizontally with a

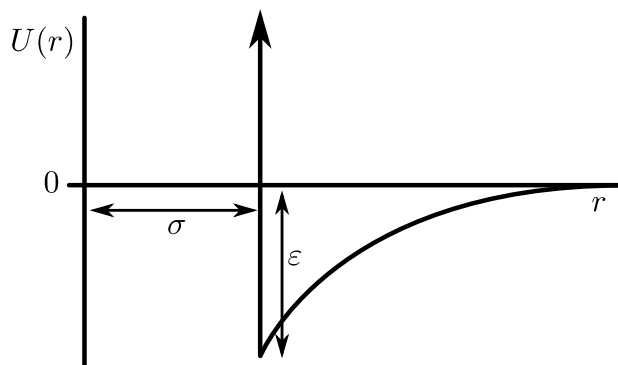


Figure 3.7: Sutherland potential

distance parameter  $\sigma$ .

The second virial coefficient is given by

$$B_2(T) = -2\pi \int_0^{\infty} r^2 (e^{-U(r)/kT} - 1) dr$$

so using the mathematical form for  $U(r)$ , the integral splits into two parts

$$\begin{aligned} B_2(T) &= 2\pi \int_0^{\sigma} r^2 dr - 2\pi \int_{\sigma}^{\infty} r^2 \left( e^{\frac{\varepsilon}{kT} \left(\frac{\sigma}{r}\right)^6} - 1 \right) dr \\ &= \frac{2}{3}\pi\sigma^3 - 2\pi \int_{\sigma}^{\infty} r^2 \left( e^{\frac{\varepsilon}{kT} \left(\frac{\sigma}{r}\right)^6} - 1 \right) dr. \end{aligned} \quad (3.2.26)$$

We substitute  $x = r/\sigma$ , so that

$$B_2(T) = \frac{2}{3}\pi\sigma^3 \left\{ 1 - 3 \int_1^{\infty} x^2 \left( e^{\frac{\varepsilon}{kT} x^{-6}} - 1 \right) dx \right\}. \quad (3.2.27)$$

This may be expressed analytically, in terms of the imaginary error function  $\operatorname{erfi}$ <sup>5</sup>:

$$B_2(T) = \frac{2}{3}\pi\sigma^3 \left( e^{\varepsilon/kT} - \sqrt{\pi} \sqrt{\frac{\varepsilon}{kT}} \operatorname{erfi} \sqrt{\frac{\varepsilon}{kT}} \right) \quad (3.2.28)$$

<sup>5</sup>The *standard* error function  $\operatorname{erf}(z)$  is an area under the Gaussian distribution function:  $\operatorname{erf}(z) = \frac{2}{\sqrt{\pi}} \int_0^z e^{-t^2} dt$ . The imaginary error function is defined as  $\operatorname{erfi}(z) = \operatorname{erf}(iz)/i$ . The *Mathematica* symbols for these are  $\operatorname{Erf}[z]$  and  $\operatorname{Erfi}[z]$ . We note that  $\operatorname{erfi}(z)$  is real for real  $z$ .

This is plotted in Fig. 3.8 together with data from nitrogen. The curve has been fitted with parameters  $\varepsilon/k = 274.2$  K,  $\sigma = 3.16$  Å. The figure also shows the hard sphere asymptote  $B_2^{\text{hs}} = 39.81$  cm<sup>3</sup>/mol. Observe that this is not such a good fit to the data.

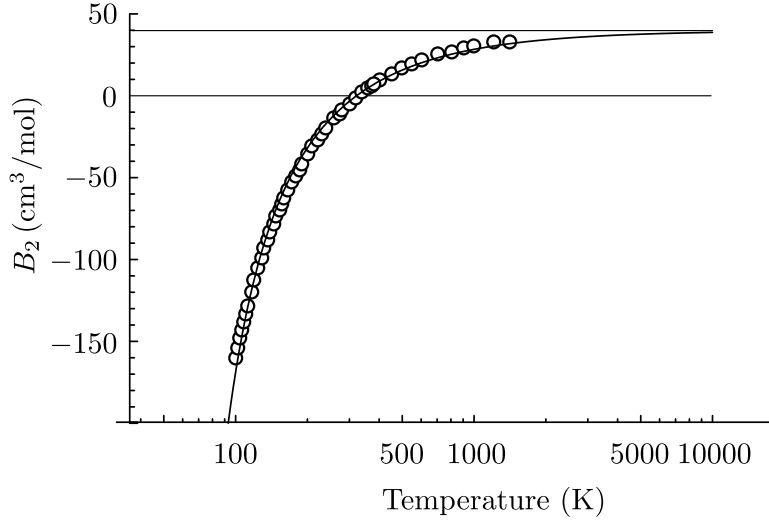


Figure 3.8: Second virial coefficient of nitrogen plotted with the Sutherland functional form, Eq. (3.2.20). Sutherland parameters  $\varepsilon/k = 274.2$  K,  $\sigma = 3.16$  Å.

The Boyle temperature for the Sutherland gas is

$$T_B = 1.171\varepsilon/k. \quad (3.2.29)$$

At high temperatures we have the series expansion

$$\begin{aligned} B_2(T) &= -\frac{2}{3}\pi\sigma^3 \sum_{n=0}^{\infty} \frac{(kT/\varepsilon)^{-n}}{n!(2n-1)} \\ &= \frac{2}{3}\pi\sigma^3 \left\{ 1 - \frac{\varepsilon}{kT} - \frac{1}{6} \left( \frac{\varepsilon}{kT} \right)^2 - \frac{1}{30} \left( \frac{\varepsilon}{kT} \right)^3 - \dots \right\} \end{aligned} \quad (3.2.30)$$

while at low temperatures we have

$$B_2(T) = -\frac{2}{3}\pi\sigma^3 e^{\varepsilon/kT} \left\{ \frac{1}{2} \frac{kT}{\varepsilon} + \frac{3}{4} \left( \frac{kT}{\varepsilon} \right)^2 + \frac{15}{8} \left( \frac{kT}{\varepsilon} \right)^3 + \dots \right\} \quad (3.2.31)$$

The interesting point about the Sutherland potential is that it gives the high-temperature behaviour of the  $B_2(T)$  as

$$B_2(T) \sim \frac{2}{3}\pi\sigma^3 \left( 1 - \frac{\varepsilon}{kT} - \dots \right); \quad (3.2.32)$$

the limiting value at high temperatures is the hard core  $2\pi\sigma^3/3$ , while the leading deviation goes as  $T^{-1}$ .

[Compare with square well potential:

$$B_2(T) \sim \frac{2}{3}\pi\sigma^3 \left( 1 - \frac{(R^3 - 1)\varepsilon}{kT} - \dots \right). \quad (3.2.33)$$

Here also the limiting high temperature value is the hard core expression and the leading deviation goes as  $T^{-1}$ . Note  $R$  is dimensionless, greater than unity. And  $\varepsilon$  is different in the two cases, i.e.

$$\varepsilon_S = (R^3 - 1)\varepsilon_{\text{sw}}. \quad (3.2.34)$$

]

By contrast, the second virial coefficient for the Lennard-Jones gas does not have such a simple high-temperature behaviour – a consequence of the “softness” of the hard core. In the high temperature limit

$$\begin{aligned} B_2(T) &\sim \frac{2}{3}\pi\sigma^3 \times \frac{2\pi}{\Gamma(1/4)} \left( \frac{\varepsilon}{kT} \right)^{1/4} \\ &\sim \frac{2}{3}\pi\sigma^3 \times 1.73 \left( \frac{\varepsilon}{kT} \right)^{1/4}, \end{aligned} \quad (3.2.35)$$

so that in this case  $B_2(t) \rightarrow 0$  as  $T \rightarrow \infty$ ; the van der Waals second virial coefficient tends to zero rather than the hard core limiting value.

### 3.2.6 Comparison of models

We plot the nitrogen second virial coefficient again, in Fig. 3.18, now showing the best fit curves corresponding to the square well, the Lennard-Jones and the Sutherland potentials. It will be observed that there is not much to choose between them. The Lennard-Jones is better than the Sutherland potential – clearly the latter is too crude. However one sees that the square well potential provides the best fit. But one should not conclude that the square well potential is the best physical model. Its better mathematical fit is simply a consequence of the fact that that model has *three* adjustable parameters, as compared with the two adjustable parameters of the Lennard-Jones and the Sutherland models.

Nevertheless, from the practical perspective the square well expression for  $B_2$  of Eq. (3.2.15) is sufficiently accurate that databases of second virial coefficients often simply give the equation’s three parameters  $A$ ,  $B$  and  $\varepsilon$ , rather than extensive tables<sup>6</sup>.

<sup>6</sup>See, for instance, the NPL Kaye and Laby web site, in particular the page <http://www.kayelaby.npl.co.uk/chemistry/3.5/3.5.html>



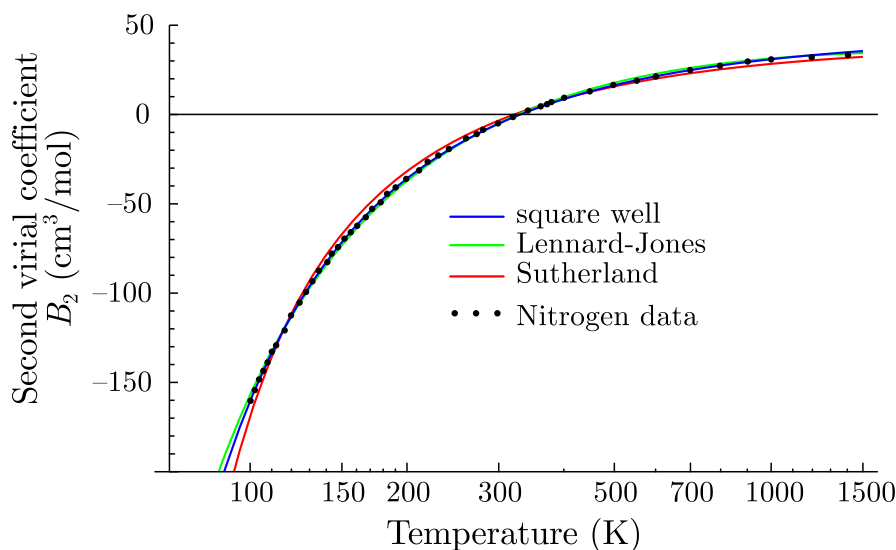


Figure 3.9: Second virial coefficient of nitrogen compared with fits corresponding to the square well, Lennard-Jones and Sutherland potentials.

The inter-particle potentials corresponding to the fits of the various models through the nitrogen  $B_2$  data are shown in Fig 3.10.

### 3.2.7 Universal behaviour

The second virial coefficient  $B_2(T)$  was obtained as an integral over the interaction energy  $U(r)$  in Eq. (3.2.2). Different gases will have different values for  $B_2(T)$  because they will have different interaction energies.

We shall make the assumption that the interaction energy may be expressed in the following way:

$$U(r) = \varepsilon u(r/\sigma). \quad (3.2.36)$$

What we are saying here is that  $U(r)$  has a universal shape and, for a given gas, it is scaled vertically by a specific energy  $\varepsilon$  and horizontally by a specific length  $\sigma$ . We note that the Lennard-Jones interaction is of this form and that values of  $\varepsilon$  and  $\sigma$  are tabulated, see for example Kittel [4].

Using this expression for  $U(r)$  in Eq. (3.2.2), by a change of variable we obtain

$$B_2/\sigma^3 = -2\pi \int_0^\infty x^2 [e^{-u(x)/\tau} - 1] dx \quad (3.2.37)$$

where  $\tau = kT/\varepsilon$  is a reduced temperature. Then to the extent that our scaling assumption for  $U(r)$  is valid, plots of  $B_2/\sigma^3$  against  $kT/\varepsilon$  would

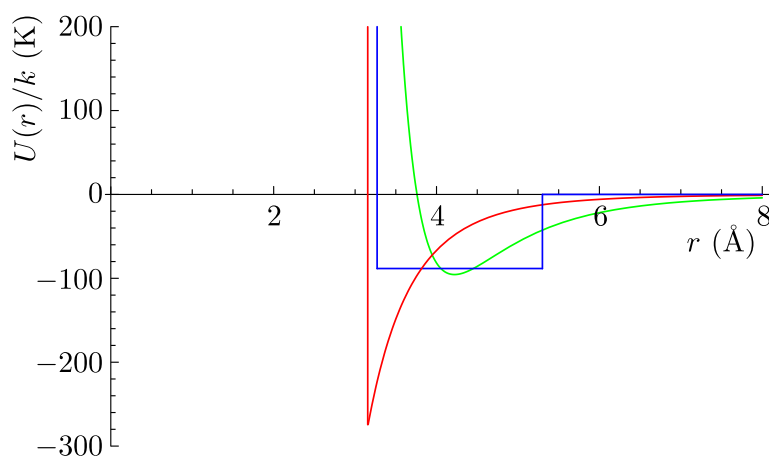


Figure 3.10: Square well, Lennard-Jones and Sutherland potentials corresponding to Nitrogen second virial coefficient fits.

fall on a single curve. In Fig. 3.11 we show such data for the noble gases, scaled with their Lennard-Jones  $\varepsilon$  and  $\sigma$ . Apart from helium, the points do indeed collapse onto a single curve. This provides support for our scaling assumption; this will be formalized into the Law of Corresponding States in the next chapter. The points in Fig. 3.11 fall very close to the curve calculated from the Lennard-Jones potential, Eq. (3.2.20).

Helium is special: because of its light mass, quantum effects are important. This is discussed in the next section.

### 3.2.8 Quantum gases – the special case(s) of helium

The main aim of this section is to explain why helium's second virial coefficient points, in Fig. 3.11, do not fall on the universal curve, which follows from the scaling property of the interaction potential. But first we shall see that a quantum gas has a non-zero  $B_2$  even in the absence of any interactions.

#### Non-interacting quantum gas

Now the second virial coefficient is a measure of the deviation from the ideal gas equation of state. But at low temperatures the equation of state for a *non-interacting* gas of quantum particles deviates from the ideal gas equation of state. We saw this in Section 2.7.1. This deviation, when expressed as a series in powers of density may be regarded as a virial expansion. This is

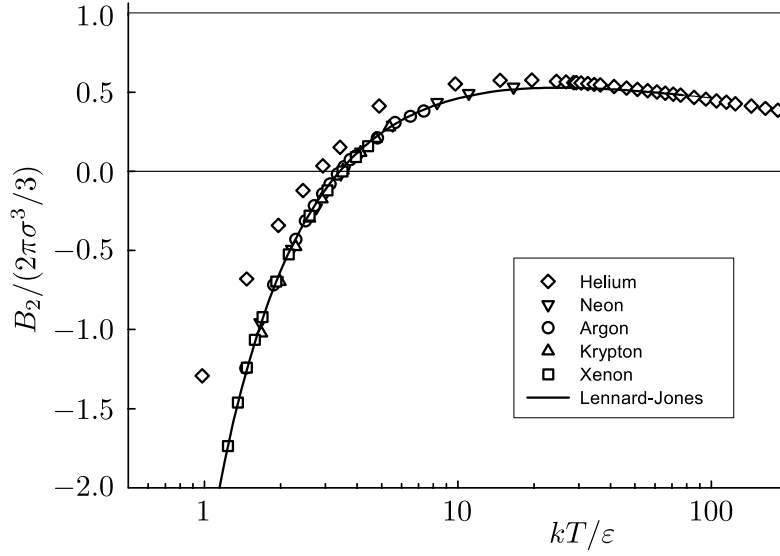


Figure 3.11: Reduced second virial coefficient of the Noble Gases, together with Lennard-Jones form. The helium data are for the abundant isotope  $^4\text{He}$ .

precisely what we did in Eq. (2.7.24), which we shall write here as

$$pV = NkT \left\{ 1 \pm \frac{\pi^{3/2}}{2\alpha} \frac{\hbar^3}{(mkT)^{3/2}} \frac{N}{V} - \frac{\pi^3}{\alpha^2} \frac{16\sqrt{3} - 27}{27} \frac{\hbar^6}{(mkT)^3} \left(\frac{N}{V}\right)^2 + \dots \right\} \quad (3.2.38)$$

where the  $+$  is for fermions and the  $-$  is for bosons, and  $\alpha$  is the spin degeneracy factor. From this expression we can directly read off the second and third virial coefficients. In particular

$$\begin{aligned} B_2^0(T) &= \pm \frac{\pi^{3/2}}{2\alpha} \frac{\hbar^3}{(mkT)^{3/2}} \\ &= \pm \frac{1}{2^{5/2}\alpha} \Lambda^3(T) \end{aligned} \quad (3.2.39)$$

where  $\Lambda$  is the thermal de Broglie wavelength, Eq. (2.3.5), and the “0” superscript indicates this is in the absence of any interaction potential.  $B_2$  is monotonic in  $T$ ; it is positive for fermions and negative for bosons. This is plotted in Fig. 3.12.

This result has an interesting interpretation. Recall the hard sphere expression for  $B_2$  was essentially the volume of a particle. Here we see that this quantum contribution to  $B_2$  is essentially the thermal deBroglie volume of the particle – positive for fermions and negative for bosons.

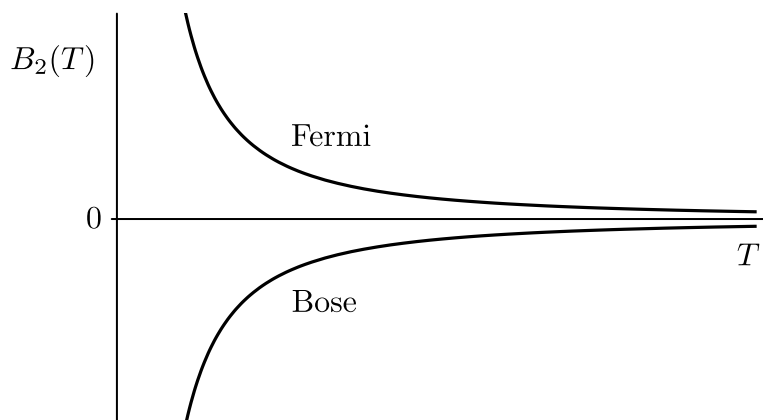


Figure 3.12: Second virial coefficient of a quantum ideal gas

It is often stated crudely that requirements of quantum statistics leads to “exchange forces” on classical “Maxwell” particles; the exclusion principle for fermions gives a repulsive force while bosons experience an attraction. Such a view can, however, be seriously misleading [5].

### Interacting quantum gas

Quantum mechanics may be regarded as influencing the second virial coefficient of a gas in two different ways. Particles are delocalized over a length scale  $\Lambda$ , and particle “statistics” will determine the symmetry of the states that are included in the partition function sum. The Lee-Yang approach to quantum statistical Mechanics [6] allows one to treat these contributions as separate and additive. We shall therefore write

$$B_2(T) = B_2^d(T) + B_2^{\text{ex}}(T) \quad (3.2.40)$$

where  $B_2^d(T)$  is the delocalization or “direct” term and  $B_2^{\text{ex}}(T)$  is the statistics or “exchange” term.

Of course a full quantum treatment will incorporate both contributions, but such calculations are rather complex and tedious [2]. Instead, we shall examine the two contributions separately. This will provide an intuitive understanding of the way quantum effects influence the second virial coefficient of the helium gases. We shall denote these two different contributions as the *statistics* and the *delocalization* contributions.

**Statistics contribution to  $B_2$** 

For non-interacting fermions or bosons there is only the statistics contribution to  $B_2$  and this is given by Eq. (3.2.39). However in the presence of interactions this is dramatically attenuated [7], so that the overwhelming effect is from the delocalization.

**Delocalization contribution to  $B_2$** 

Quantum mechanics may be regarded as causing a delocalization of the atomic positions and this may be accommodated by a renormalization of the inter-atomic interaction. This idea was suggested by Feynman [8] and subsequently the procedure was developed by Young [9] for the case of the Lennard-Jones interaction. Essentially one averages the interaction potential over a Gaussian probability density whose width is the thermal de Broglie wavelength. The result is a Lennard-Jones interaction with renormalized  $\varepsilon$  and  $\sigma$  which depend on temperature. We shall simply quote the result, and refer the interested reader to the original references for the details.

In terms of the Lennard-Jones parameters  $\varepsilon$  and  $\sigma$ , we define a characteristic temperature  $T^*$ :

$$T^* = \frac{1}{6\pi} \frac{\hbar}{k\sigma} \sqrt{\frac{\varepsilon}{m}} \quad (3.2.41)$$

in terms of which we can introduce a reduced temperature variable  $\tau$

$$\tau = T/T^*. \quad (3.2.42)$$

Then the renormalization of the Lennard-Jones  $\varepsilon$  and  $\sigma$  is given, in terms of the reduced temperature, by:

$$\begin{aligned} \varepsilon &\rightarrow \bar{\varepsilon}(\tau) = \mathcal{E}(\tau)\varepsilon \\ \sigma &\rightarrow \bar{\sigma}(\tau) = \mathcal{S}(\tau)\sigma \end{aligned} \quad (3.2.43)$$

where

$$\begin{aligned} \mathcal{E}(\tau) &= [1 + 19.1\tau^{-1} + f(\tau)\tau^{-2}]^{-3/4} \\ \mathcal{S}(\tau) &= [1 + g(\tau)\tau^{-1}]^{1/2}. \end{aligned} \quad (3.2.44)$$

and

$$\begin{aligned} f(\tau) &= 5 + (177.7 - 5) [1 - e^{-\tau/250}] \\ g(\tau) &= 4 + (7.54 - 4) [1 - e^{-\tau/250}] \end{aligned} \quad (3.2.45)$$

These quantum renormalization factors are shown, as a function of reduced temperature  $\tau$  in Fig. 3.14

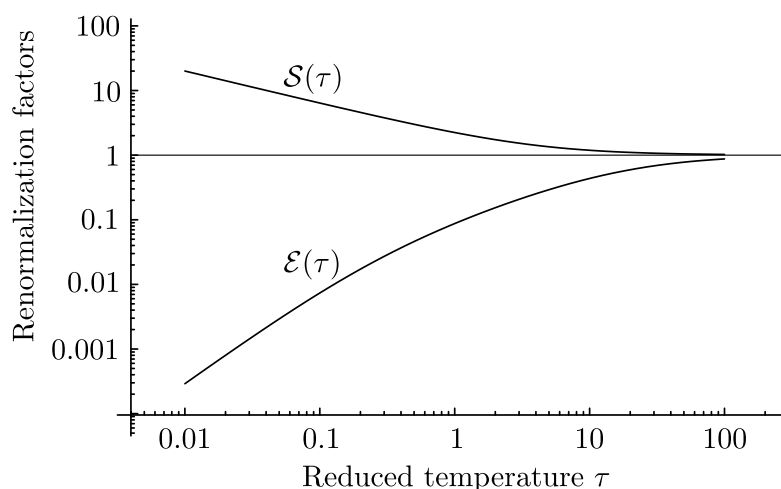


Figure 3.13: Quantum renormalization factors for the Lennard-Jones  $\sigma$  and  $\varepsilon$  parameters.

### Consequences for Helium

There are two isotopes of helium: the abundant and heavier  $^4\text{He}$  and the rarer and lighter  $^3\text{He}$ . We note that  $^4\text{He}$  is a boson and  $^3\text{He}$  is a fermion. I have plotted  $B_2$  data for the helium isotopes in Fig. 3.14 together with the Lennard-Jones curve, as in Fig. 3.11.

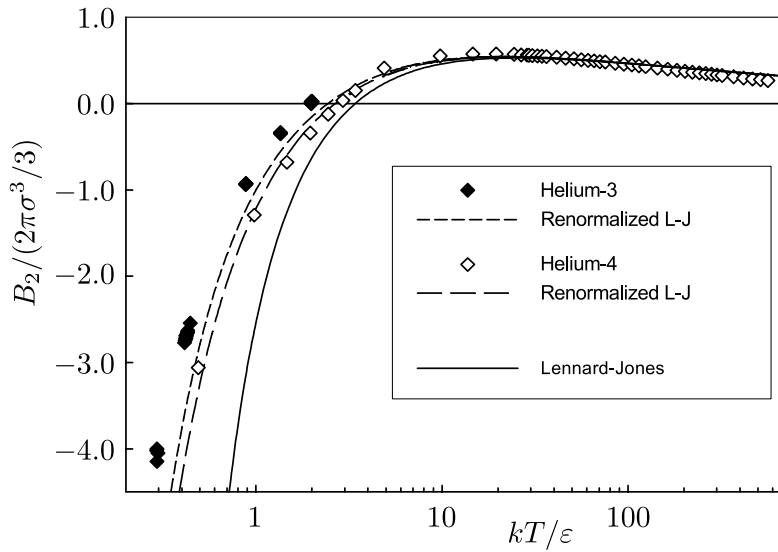
While the Lennard-Jones parameters for the two isotopes will be the same, since they have different masses, the renormalization factors will be different. By applying these renormalizations to the  $\varepsilon$  and  $\sigma$  in Eq. (3.2.20) we obtain the two dashed curves in Fig. 3.14. The bare Lennard-Jones curve has been shifted *almost* through the data points.

From this we conclude that delocalization effect almost accounts for the second virial coefficients of  $^3\text{He}$  and  $^4\text{He}$ . The difference between  $B_2$  for the two isotopes is predominantly because of their different masses and not because of their different statistics.

## 3.3 Thermodynamics

### 3.3.1 Throttling

In a throttling process a gas is forced through a flow impedance such as a porous plug. For a continuous process, in the steady state, the pressure will be constant (but different) either side of the impedance. When this happens to a thermally isolated system so that heat neither enters nor leaves the sys-

Figure 3.14: Second virial coefficient of  ${}^3\text{He}$  and  ${}^4\text{He}$ .

tem then it is referred to as a Joule-Kelvin or Joule Thompson process. This is fundamentally an irreversible process, but the arguments of thermodynamics are applied to such a system simply by considering the equilibrium initial state and the equilibrium final state which applied way before and way after the actual process. This throttling process may be modelled by the diagram in Fig. 3.15.

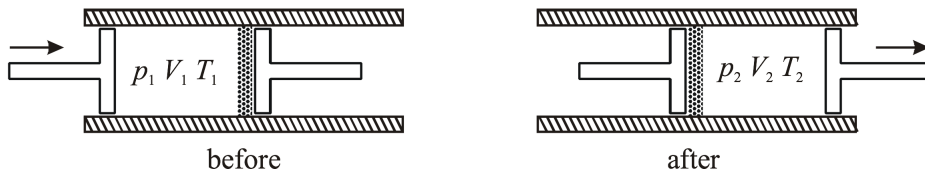


Figure 3.15: Joule-Kelvin throttling process

Work must be done to force the gas through the plug. The work done is

$$\Delta W = - \int_{V_1}^0 p_1 dV - \int_0^{V_2} p_2 dV = p_1 V_1 - p_2 V_2. \quad (3.3.1)$$

Since the system is thermally isolated the change in the internal energy is due entirely to the work done:

$$E_2 - E_1 = p_1 V_1 - p_2 V_2 \quad (3.3.2)$$

or

$$E_1 + p_1 V_1 = E_2 + p_2 V_2. \quad (3.3.3)$$

The *enthalpy*  $H$  is defined by

$$H = E + pV \quad (3.3.4)$$

thus we conclude that in a Joule-Kelvin process the enthalpy is conserved.

The interest in the throttling process is that whereas for an ideal gas the temperature remains constant, it is possible to have either cooling or warming when the process happens to a non-ideal gas. The operation of most refrigerators is based on this.

### 3.3.2 Joule-Thomson coefficient

The fundamental differential relation for the enthalpy is

$$dH = TdS + Vdp. \quad (3.3.5)$$

It is, however, rather more convenient to use  $T$  and  $p$  as the independent variables rather than the natural  $S$  and  $p$ . This is effected by expressing the entropy as a function of  $T$  and  $p$  whereupon its differential may be expressed as

$$dS = \left. \frac{\partial S}{\partial T} \right|_p dT + \left. \frac{\partial S}{\partial p} \right|_T dp. \quad (3.3.6)$$

But

$$\left. \frac{\partial S}{\partial T} \right|_p = \frac{c_p}{T} \quad (3.3.7)$$

and using a Maxwell relation we have

$$\left. \frac{\partial S}{\partial p} \right|_T = - \left. \frac{\partial V}{\partial T} \right|_p \quad (3.3.8)$$

so that

$$dH = c_p dT + \left\{ V - T \left. \frac{\partial V}{\partial T} \right|_p \right\} dp. \quad (3.3.9)$$

Now since  $H$  is conserved in the throttling process  $dH = 0$  so that

$$dT = \frac{1}{c_p} \left\{ T \left. \frac{\partial V}{\partial T} \right|_p - V \right\} dp \quad (3.3.10)$$

which tells us how the temperature change is determined by the pressure change. The *Joule-Thomson* coefficient  $\mu_J$  is defined as the derivative

$$\mu_J = \left. \frac{\partial T}{\partial p} \right|_H, \quad (3.3.11)$$



giving

$$\mu_J = \frac{1}{c_p} \left\{ T \left. \frac{\partial V}{\partial T} \right|_p - V \right\} \quad (3.3.12)$$

This is zero for the ideal gas (Problem 3.1). When  $\mu_J$  is positive then the temperature decreases in a throttling process when a gas is forced through a porous plug.

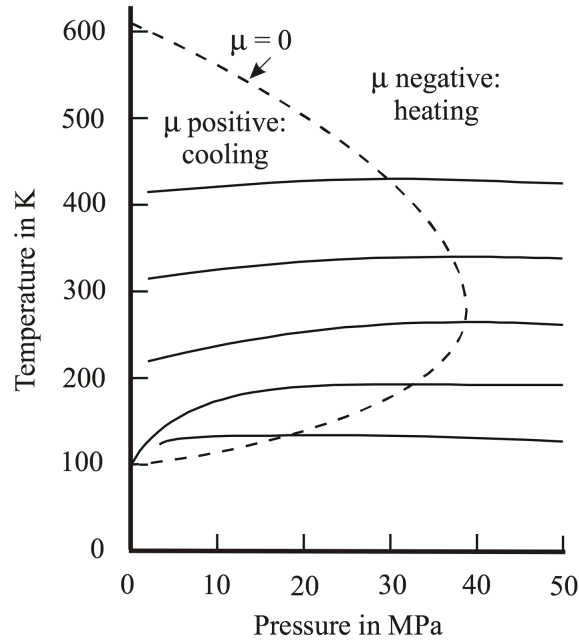


Figure 3.16: Isenthalps and inversion curve for nitrogen (after Zemansky[10])

### 3.3.3 Connection with the second virial coefficient

We consider the case where the second virial coefficient gives a good approximation to the equation of state. Then we are assuming that the density is low enough so that the third and higher coefficients can be ignored. This means that the second virial coefficient correction to the ideal gas equation is small and then solving for  $V$  in the limit of small  $B_2(T)$  gives

$$V = \frac{NkT}{p} + NB_2(T). \quad (3.3.13)$$

so that the Joule-Thomson coefficient is then

$$\mu_J = \frac{NT}{c_p} \left\{ \frac{dB_2(T)}{dT} - \frac{B_2(T)}{T} \right\}. \quad (3.3.14)$$

Within the low density approximation it is appropriate to use the ideal gas thermal capacity

$$c_p = \frac{5}{2}Nk \quad (3.3.15)$$

so that

$$\mu_J = \frac{2T}{5k} \left\{ \frac{dB_2(T)}{dT} - \frac{B_2(T)}{T} \right\}. \quad (3.3.16)$$

### 3.3.4 Inversion temperature

The behaviour of the Joule-Thomson coefficient can be seen from the following construction. We take the shape of  $B_2(T)$  from the square well potential model. While not qualitatively correct, this does exhibit the general features of a realistic interparticle potential.

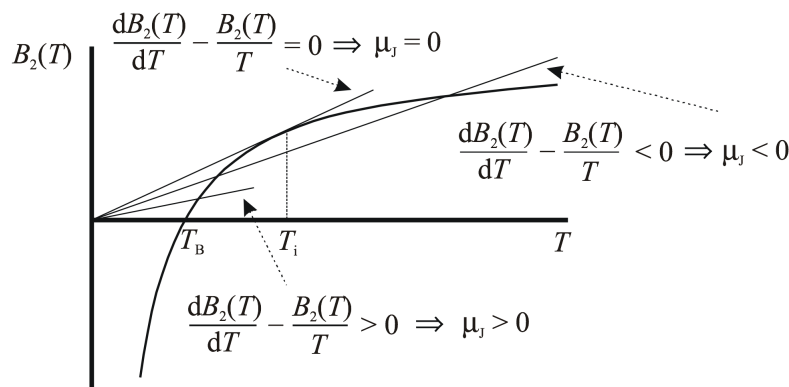


Figure 3.17: Behaviour of the Joule-Thomson coefficient

We see that at low temperatures the slope of the curve,  $dB/dT$  is greater than  $B/T$  so that  $\mu_J$  is positive, while at high temperatures the slope of the curve,  $dB/dT$  is less than  $B/T$  so that  $\mu_J$  is negative. The temperature where  $\mu_J$  changes sign is called the *inversion temperature*,  $T_i$ .

The inversion curve for nitrogen is shown as the dashed line in Fig. 3.16. We see that at high temperatures  $\mu_J$  is negative, as expected. As the temperature is decreased the inversion curve is crossed and  $\mu_J$  becomes positive. Note, however that the the low density approximation, implicit in going only to the *second* virial coefficient, keeps us away from the lower temperature region where the gas is close to condensing, where the Joule-Thomson coefficient changes sign again.

## Sutherland bit

The Boyle temperature and the inversion temperature for this gas may be found from their definitions

$$\begin{aligned} B_2(T) = 0 &\quad \rightarrow \quad T_B \\ \frac{dB_2(T)}{dT} - \frac{B_2(T)}{T} = 0 &\quad \rightarrow \quad T_i \end{aligned} \quad (3.3.17)$$

to give

$$\begin{aligned} T_B &= 1.171\varepsilon/k \\ T_i &= 2.215\varepsilon/k. \end{aligned} \quad (3.3.18)$$

The tangent construction for the inversion temperature (Section 3.3.4 and Fig. 3.8) is shown in Fig. 3.18. The ratio is then

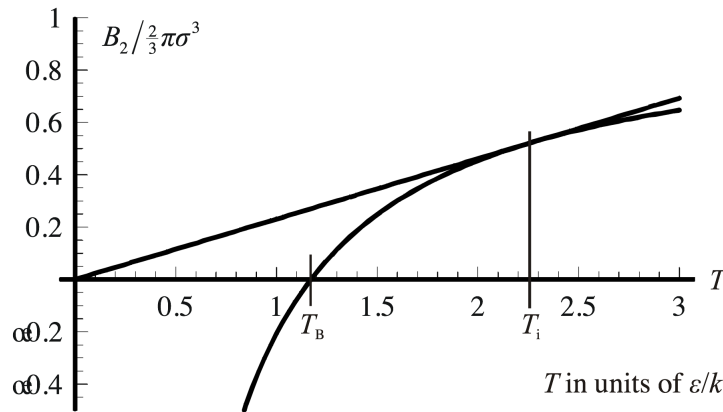


Figure 3.18: Boyle temperature and inversion temperature

$$T_i/T_B = 1.259. \quad (3.3.19)$$

## 3.4 Van der Waals Equation of State

### 3.4.1 Approximating the Partition Function

Rather than perform an exact calculation as a series in powers of an expansion parameter – the density or the cluster function  $f_{ij}$  – in this section we shall adopt a different approach by making an approximation to the partition

function, which should be reasonably valid at *all* densities. Furthermore the approximation we shall develop will be based on the single-particle partition function. We shall, in this way, obtain an equation of state that approximates the behaviour of real gases. This equation was originally proposed by van der Waals in his Ph.D. Thesis in 1873. An English translation is available [11] and it is highly readable; van der Waals's brilliance shines out.

In the absence of an interaction potential the single-particle partition function is

$$z = \frac{V}{\Lambda^3}. \quad (3.4.1)$$

Recall that the factor  $V$  here arises from integration over the position coordinates. The question now is how to account for the inter-particle interactions – in an approximate way. Now the interaction  $U(r)$  comprises a strong repulsive hard core at short separations and a weak attractive long tail at large separations. And the key is to treat these two parts of the interaction in separate ways.

- The repulsive core effectively excludes regions of space from the integration over position coordinates. This may be accounted for by replacing  $V$  by  $V - V_{\text{ex}}$  where  $V_{\text{ex}}$  is the volume excluded by the repulsive core.
- The attractive long tail is accounted for by including a factor in the expression for  $z$  of the form

$$e^{-\langle E \rangle / kT} \quad (3.4.2)$$

where  $\langle E \rangle$  is an average of the attractive part of the potential.

Thus we arrive at the approximation

$$z = \frac{V - V_{\text{ex}}}{\Lambda^3} e^{-\langle E \rangle / kT}. \quad (3.4.3)$$

Note that we have approximated the interaction by a *mean field* assumed to apply to individual particles. This allows us to keep the simplifying feature of the free-particle calculation where the many-particle partition function factorises into a product of single-particle partition functions. This is accordingly referred to as a mean field calculation.

### 3.4.2 Van der Waals Equation

The equation of state is found by differentiating the free energy expression:

$$p = kT \left. \frac{\partial \ln Z}{\partial V} \right|_{T,N} = NkT \left. \frac{\partial \ln z}{\partial V} \right|_T. \quad (3.4.4)$$

Now the logarithm of  $z$  is

$$\ln z = \ln(V - V_{\text{ex}}) - 3 \ln \Lambda - \langle E \rangle / kT \quad (3.4.5)$$

so that

$$p = NkT \left. \frac{\partial \ln z}{\partial V} \right|_T = \frac{NkT}{V - V_{\text{ex}}} - N \frac{d\langle E \rangle}{dV} \quad (3.4.6)$$

since we allow the average interaction energy to depend on volume (density). This equation may be rearranged as

$$p + N \frac{d\langle E \rangle}{dV} = \frac{NkT}{V - V_{\text{ex}}} \quad (3.4.7)$$

or

$$\left( p + N \frac{d\langle E \rangle}{dV} \right) (V - V_{\text{ex}}) = NkT. \quad (3.4.8)$$

This is similar to the ideal gas equation except that the pressure is increased and the volume decreased from the ideal gas values. These are constant parameters. They account, respectively, for the attractive long tail and the repulsive hard core in the interaction. Conventionally we express the parameters as  $aN^2/V^2$  and  $Nb$ , so that the equation of state is

$$\left( p + a \frac{N^2}{V^2} \right) (V - Nb) = NkT \quad (3.4.9)$$

and this is known as the van der Waals equation.

Some isotherms of the van der Waals equation are plotted in Fig. 3.19 for three temperatures  $T_1 > T_2 > T_3$ . On the right hand side of the plot, corresponding to low density, we have gaseous behaviour; here the van der Waals equation gives small deviations from the ideal gas behaviour. On the left hand side, particularly at the lower temperatures, the steep slope indicates incompressibility. This is indicative of liquid behaviour. The non-monotonic behaviour at low temperature is peculiar and indeed it is non-physical. This will be discussed in detail in the next chapter.

The van der Waals equation gives a good description of the behaviour of both gases and liquids. In introducing this equation of state we said that the method should treat both low-density and high-density behaviour, and this it has done admirably. For this reason Landau and Lifshitz [12] refer to the van der Waals equation as an interpolation equation. The great power of the equation, however, is that it also gives a good *qualitative* description of the gas-liquid phase transition, to be discussed in Chapter 4.

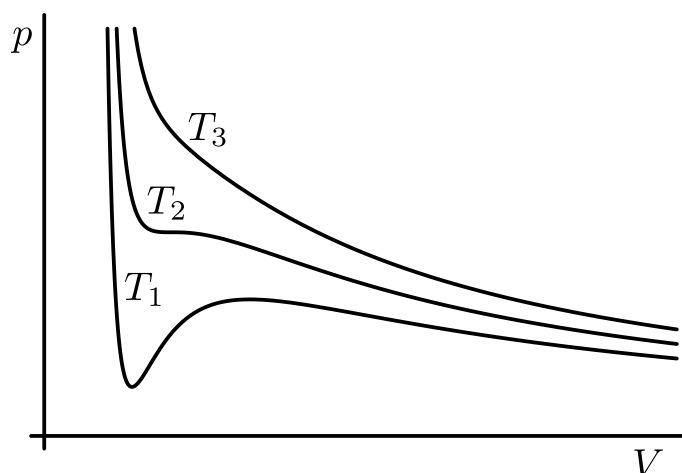


Figure 3.19: van der Waals isotherms

### 3.4.3 Estimation of van der Waals Parameters

In the van der Waals approach the repulsive and the attractive parts of the inter-particle interaction were treated separately. Within this spirit let us consider how the two parameters of the van der Waals equation might be related to the two parameters of the Lennard-Jones inter-particle interaction potential. The repulsion is strong; particles are correlated when they are very close together. We accounted for this by saying that there is zero probability of two particles being closer together than  $\sigma$ . Then, as in the hard core discussion of Section 3.2.1, the region of co-ordinate space is excluded, and the form of the potential in the excluded region ( $U(r)$  very large) does not enter the discussion. Thus just as in the discussion of the hard core model, the excluded volume will be

$$V_{\text{ex}} = \frac{2}{3}N\pi\sigma^3. \quad (3.4.10)$$

The attractive part of the potential is weak. Here there is very little correlation between the positions of the particles; we therefore treat their distribution as approximately uniform. The mean interaction for a single pair of particles  $\langle E_p \rangle$  is then

$$\begin{aligned} \langle E_p \rangle &= \frac{1}{V} \int_{\sigma}^{\infty} 4\pi r^2 U(r) dr \\ &= \frac{1}{V} \int_{\sigma}^{\infty} 4\pi r^2 4\epsilon \left\{ \left( \frac{\sigma}{r} \right)^{12} - \left( \frac{\sigma}{r} \right)^6 \right\} dr \\ &= -\frac{32\pi\sigma^3}{9V} \epsilon. \end{aligned} \quad (3.4.11)$$

Now there are  $N(N-1)/2$  pairs, each interacting through  $U(r)$ , so neglecting the 1, the total energy of interaction is  $N^2 \langle E_p \rangle / 2$ . This is shared among the  $N$  particles, so the mean energy per particle is

$$\begin{aligned} \langle E \rangle &= \langle E_p \rangle N / 2 \\ &= -\frac{16\pi\sigma^3 N}{9} \frac{N}{V} \varepsilon. \end{aligned} \quad (3.4.12)$$

In the van der Waals equation it is the derivative of this quantity we require. Thus we find

$$N \frac{d\langle E \rangle}{dV} = \frac{16}{9} \pi \sigma^3 \left( \frac{N}{V} \right)^2 \varepsilon. \quad (3.4.13)$$

These results give the correct assumed  $N$  and  $V$  dependence of the parameters used in the previous section. So finally we identify the van der Waals parameters  $a$  and  $b$  as

$$\begin{aligned} a &= \frac{16}{9} \pi \sigma^3 \varepsilon \\ b &= \frac{2}{3} \pi \sigma^3. \end{aligned} \quad (3.4.14)$$

### 3.4.4 Virial Expansion

It is a straightforward matter to expand the van der Waals equation as a virial series. We express  $p/kT$  as

$$\begin{aligned} \frac{p}{kT} &= \frac{N}{V - Nb} - \frac{aN^2}{kTV^2} \\ &= \left( \frac{N}{V} \right) \left( 1 - b \frac{N}{V} \right)^{-1} - \frac{a}{kT} \left( \frac{N}{V} \right)^2 \end{aligned} \quad (3.4.15)$$

and this may be expanded in powers of  $N/V$  to give

$$\frac{p}{kT} = \left( \frac{N}{V} \right) + \left( \frac{N}{V} \right)^2 \left( b - \frac{a}{kT} \right) + \left( \frac{N}{V} \right)^3 b^2 + \left( \frac{N}{V} \right)^4 b^3 + \dots \quad (3.4.16)$$

Thus we immediately identify the second virial coefficient as

$$B_2^{\text{VW}}(T) = b - \frac{a}{kT}. \quad (3.4.17)$$

This has the form as sketched for the square well potential. For this model we can find the Boyle temperature and the inversion temperature:

$$\begin{aligned} T_B &= \frac{a}{bk}, \\ T_i &= \frac{2a}{bk}. \end{aligned} \quad (3.4.18)$$

So we conclude that for the van der Waals gas the inversion temperature is double the Boyle temperature.

Incidentally, we observe that the third and all higher virial coefficients, within the van der Waals model, are constants independent of temperature.

## 3.5 Other Phenomenological Equations of State

### 3.5.1 The Dieterici equation

The Dieterici equation of state is one of a number of phenomenological equations crafted to give reasonable agreement with the behaviour of real gases. The interest in the Dieterici is twofold.

1. The equation gives a better description of the behaviour of fluids in the vicinity of the critical point than does the van der Waals equation. This will be discussed in Chapter 4, in Section 4.2.
2. The equation is consistent with the Third Law of Thermodynamics [13].

The Dieterici equation may be written as

$$p(V - Nb) = NkTe^{-\frac{Na}{kTV}}. \quad (3.5.1)$$

As with the van der Waals equation, this equation has two parameters,  $a$  and  $b$ , that parameterise the deviation from ideal gas behaviour.

For the present we briefly examine the virial expansion of the Dieterici equation. In other words we will look at the way this equation treats the initial deviations from the ideal gas.

#### Virial expansion

In order to obtain the virial expansion we express the Dieterici equation as

$$\frac{p}{kT} = \frac{N}{V - Nb} e^{-\frac{Na}{kTV}}. \quad (3.5.2)$$

And from this we may expand to give the series in  $N/V$

$$\frac{p}{kT} = \frac{N}{V} + \left(\frac{N}{V}\right)^2 \left(b - \frac{a}{kT}\right) + \left(\frac{N}{V}\right)^3 \left(b^2 - \frac{a^2}{2k^2T^2} - \frac{ab}{kT}\right) + \dots \quad (3.5.3)$$

This gives the second virial coefficient to be

$$B_2^D = b - \frac{a}{kT}. \quad (3.5.4)$$



This is the same as that for the van der Waals gas, and the parameters  $a$  and  $b$  may thus be identified with those of the van der Waals model. As a consequence, we conclude that both the van der Waals gas and the Dieterici gas have the same values for the Boyle temperature and the inversion temperature.

The third virial coefficient is given by

$$B_3^D(T) = b^2 - \frac{a^2}{2k^2T^2} - \frac{ab}{kT}; \quad (3.5.5)$$

we see that this depends on temperature, unlike that for the van der Waals equation, which is temperature-independent.

### 3.5.2 The Berthelot equation

As with the Dieterici equation, the Berthelot equation is another of phenomenological origin. The equation is given by

$$\left(p + \frac{\alpha N^2}{kTV^2}\right)(V - Nb) = NkT. \quad (3.5.6)$$

The parameters of the Berthelot equation are given by  $\alpha$  and  $b$ . We observe this equation is very similar to the van der Waals equation; there is a slight difference in the pressure-correction term that accounts for the long distance attraction of the intermolecular potential.

Since the Berthelot and van der Waals equation are related by  $a = \alpha/kT$  it follows that the Berthelot second virial coefficient is given by

$$B_2^B = b - \frac{\alpha}{(kT)^2}. \quad (3.5.7)$$

### 3.5.3 The Redlich-Kwong equation

Most improved phenomenological equations of state involve the introduction of additional parameters. The Redlich-Kwong equation is as good as many multi-parameter equations but, as with the previous equations we have considered, it has only two parameters. We shall write the Redlich-Kwong equation as

$$p = \frac{NkT}{V - Nb} - \frac{aN^2}{\sqrt{kT}V(V + Nb)}. \quad (3.5.8)$$

This should be compared to the similar expression for the van der Waals equation, Eq. (3.4.15).

The virial expansion is

$$\frac{p}{kT} = \frac{N}{V} + \left(\frac{N}{V}\right)^2 \left(b - \frac{a}{(kT)^{3/2}}\right) + \left(\frac{N}{V}\right)^3 \left(b^2 + \frac{ab}{(kT)^{3/2}}\right) + \dots \quad (3.5.9)$$

so, in particular, we identify the Redlich-Kwong second virial coefficient to be

$$B_2^{\text{RK}} = b - \frac{a}{(kT)^{3/2}} \quad (3.5.10)$$

(note:  $kT_c = 0.345(a/b)^{2/3}$ ,  $V_c = 3.847Nb$ ,  $p_c = 0.02989a^{2/3}/b^{5/3}$ )

## 3.6 Hard Sphere Gas

The interactions between the atoms or molecules of a real gas comprise a strong repulsion at short distances and a weak attraction at long distances. Both of these are important in determining how the properties of the gas differ from those of an ideal (non-interacting) gas. We have already considered various approximations to the inter-particle interaction when we looked at initial deviations from ideal behaviour in the calculations of the virial expansions in Section 3.2. We considered a sequence of model approximations from the simplest: the hard core potential, to the most realistic: the Lennard-Jones 6-12 potential.

In this section we shall return for a deeper study of the to the hard core potential. In justification we can do no better than to quote from Chaikin and Lubensky[14] p.40: “Although this seems like an immense trivialisation of the problem, there is a good deal of unusual and unexpected physics to be found in hard-sphere models.”

We recall that the hard core potential, Eq. (3.2.3) is

$$\begin{aligned} U(r) &= \infty & r < \sigma \\ &= 0 & r > \sigma \end{aligned}$$

where  $\sigma$  is the hard core diameter. This is indeed a simplification of a real inter-particle interaction – but what behaviour does it predict? What properties of real systems can be understood in terms of the short-distance repulsion? And, indeed, what properties cannot be understood from this simplification?

### 3.6.1 Possible approaches

The direct way of solving the problem of the hard sphere fluid would be to evaluate the partition function; everything follows from that. Even for an

interaction as simple as this, it turns out that the partition function cannot be evaluated analytically except in one dimension; this is the so-called Tonks hard stick model, which leads to the (one-dimensional) Clausius equation of state

$$p(L - L_{\text{ex}}) = NkT. \quad (3.6.1)$$

Certainly in two and three dimensions no explicit solution is possible.<sup>7</sup> Arguments about why the partition function (really the configuration integral) is so difficult to evaluate are given in Reif [15]. The point is that the excluded volumes appear in nested integrals and these are impossible to untangle, except in one dimension. Accepting that no analytic solution is possible in three dimensions, there is a number of approaches that might be considered.

- Mean field – this will indicate the general behaviour to be expected,
- Virial expansion – this represents first-principles theoretical calculation.
- Molecular dynamics – this may be viewed as accurate “measurements made by computer”.

The mean field approach<sup>8</sup> to the the hard sphere gas results in the Clausius equation of state: the ideal gas equation, but with an excluded volume term.

$$p(V - V_{\text{ex}}) = NkT. \quad (3.6.2)$$

This follows by analogy with our treatment of the van der Waals gas, where now there is no attractive term in the interaction. See also Problem 3.8.

There are extensive molecular dynamics simulations, see in particular Bannerman *et al.*[16] and it is even possible to do your own; the applications of Gould and Tobochnik [17] are very instructive for this.

We shall look at virial expansions and see how far they may be “pushed”. In other words our interest is in what *analytical* conclusions may be drawn. We can then compare these conclusions with the molecular dynamics “experimental data”.

---

<sup>7</sup>(Question: is “excluded volume” treatment a mean-field treatment – and so is the excluded volume argument then valid for four and higher dimensions? This can be tested using the virial coefficients calculated by Clisby and McCoy for four and higher dimensions. – The answer is NO; strictly speaking “excluded volume” is not part of the mean field procedure)

<sup>8</sup>But see footnote above – this is not truly a mean field procedure.

### 3.6.2 Hard Sphere Equation of state

The equation of state of a hard-sphere fluid has a very special form. Recall that the Helmholtz free energy  $F$  is given in terms of the partition function  $Z$  by

$$F = -kT \ln Z. \quad (3.6.3)$$

We saw that the partition function for an interacting gas may be written as

$$Z = Z_{\text{id}} Q \quad (3.6.4)$$

where  $Z_{\text{id}}$  is the partition function for an ideal (non-interacting) gas

$$Z = \frac{1}{N!} \left( \frac{V}{\Lambda^3} \right)^N \quad (3.6.5)$$

and  $Q$  is the configuration integral

$$Q = \frac{1}{V^N} \int e^{-(\sum_{i<j} U(q_i, q_j))/kT} d^{3N}q. \quad (3.6.6)$$

To obtain the equation of state we must find the pressure, by differentiating the free energy

$$\begin{aligned} p &= - \left. \frac{\partial F}{\partial V} \right|_{T,N} \\ &= kT \left. \frac{\partial \ln Z}{\partial V} \right|_{T,N} \\ &= kT \left( \left. \frac{\partial \ln Z_{\text{id}}}{\partial V} \right|_{T,N} + \left. \frac{\partial \ln Q}{\partial V} \right|_{T,N} \right). \end{aligned} \quad (3.6.7)$$

It is important, now, to appreciate that the configuration integral is independent of temperature. This must be so, since there is no energy scale for the problem; the interaction energy is either zero or it is infinite. Thus the ratio  $E/kT$  will be temperature-independent. The pressure of the hard-sphere gas must then take the form

$$p = kT \left( \frac{N}{V} + g(N/V) \right). \quad (3.6.8)$$

The function  $g(N/V)$  is found by differentiating  $\ln Q$  with respect to  $V$ . We know it is a function of  $N$  and  $V$  and in the thermodynamic limit the argument must be intensive. Thus the functional form, and we have the low-density ideal gas limiting value  $g(0) = 0$ .

The important conclusion we draw from these arguments, and in particular from Eq. (3.6.8) is that for a hard sphere gas the combination  $p/kT$  is a function of the density  $N/V$ . This function must depend also on the only parameter of the interaction: the hard core diameter  $\sigma$ .

### 3.6.3 Virial Expansion

The virial expansion, Eq. (3.2.1), is written as

$$\frac{p}{kT} = \frac{N}{V} + B_2 \left(\frac{N}{V}\right)^2 + B_3 \left(\frac{N}{V}\right)^3 + \dots \quad (3.6.9)$$

where the virial coefficients  $B_m$  are, in the general case, functions of temperature. However, as argued above, for the hard sphere gas the virial coefficients are temperature-independent.

The virial expansion may be regarded as a low-density approximation to the equation of state. Certainly this is the case when only a finite number of coefficients is available. If, however, *all* the coefficients were known, then provided the series were convergent, the sum would give  $p/kT$  for all values of the density  $N/V$  up to the radius of convergence of the series : the complete equation of state. Now although we are likely to know the values for but a finite number of the virial coefficients, there may be ways of guessing / inferring / estimating the higher-order coefficients. We shall examine two ways of doing this.

### 3.6.4 Virial Coefficients

The second virial coefficient for the hard sphere gas was calculated in Section 3.2.2; we found

$$B_2 = \frac{2}{3}\pi\sigma^3, \quad (3.6.10)$$

independent of temperature, as expected.

The general term of the virial expansion is  $(\frac{N}{V})^m B_m$ , which must have the dimensions of  $N/V$ . Thus  $B_m$  will have the dimensions of  $V^{m-1}$ . Now the only variable that the hard sphere virial coefficients depend on is  $\sigma$ . Thus it is clear that

$$B_m = \text{const} \times \sigma^{3(m-1)} \quad (3.6.11)$$

where the constants are dimensionless numbers – which must be determined.

It is increasingly difficult to calculate the higher-order virial coefficients; the second and third were calculated by Boltzmann in 1899; those up to sixth order were evaluated by Ree and Hoover[18] in 1964, and terms up to tenth order were found by Clisby and McCoy[19] in 2006. More recently the eleventh and twelfth were obtained by Wheatley in 2013[20]. These all are listed in the table below, in terms of the single parameter  $b$ :

$$b = B_2 = \frac{2}{3}\pi\sigma^3. \quad (3.6.12)$$

$B_2/b$	=	1
$B_3/b^2$	=	0.625
$B_4/b^3$	=	0.28694950
$B_5/b^4$	=	0.11025210
$B_6/b^5$	=	0.03888198
$B_7/b^6$	=	0.01302354
$B_8/b^7$	=	0.00418320
$B_9/b^8$	=	0.00130940
$B_{10}/b^9$	=	0.00040350
$B_{11}/b^{10}$	=	0.00012300
$B_{12}/b^{11}$	=	0.00003700

Table 3.1: Virial coefficients for the hard sphere gas.  $B_2$  and  $B_3$  calculated by Boltzmann,  $B_4$  to  $B_6$  by Ree and Hoover,  $B_7$  to  $B_{10}$  by Clisby and McCoy.

Note/recall that the hard sphere virial coefficients are independent of temperature (Problem 3.7) and they are all expressed in terms of the hard core dimension.

We now consider ways of guessing / inferring / estimating the higher-order coefficients, so that the hard sphere equation of state may be approximated.

### 3.6.5 Carnahan and Starling procedure

We start with the remarkable procedure of Carnahan and Starling[21]. They inferred a general (approximate) expression for the  $n$ th virial coefficient, enabling them to sum the virial expansion and thus obtain an equation of state in *closed form*. The virial expansion is written as

$$\frac{pV}{NkT} = 1 + B_2 \left( \frac{N}{V} \right) + B_3 \left( \frac{N}{V} \right)^2 + \dots \quad (3.6.13)$$

In 1969 only the first six virial coefficients, from Ree and Hoover, were known. Carnahan and Starling specified the density as the fraction of the volume occupied by the spheres. The volume of a sphere of diameter  $\sigma$  is  $\frac{1}{6}\pi\sigma^3$  or  $b/4$ . So the packing fraction  $y$  is given by  $y = Nb/4V$  in terms of which Carnahan and Starling wrote the virial expansion as<sup>9</sup>

$$\frac{pV}{NkT} = 1 + 4y + 10y^2 + 18.36y^3 + 28.22y^4 + 39.82y^5 + \dots \quad (3.6.14)$$

<sup>9</sup>Actually Carnahan and Starling had a slight, but insignificant error in their final term's coefficient; Ree and Hoover's  $B_6$  was not quite right.

It is convenient to introduce “reduced” virial coefficients  $\beta_n$  such that Carnahan and Starling series is

$$\frac{pV}{NkT} = 1 + \beta_2 y + \beta_3 y^2 + \cdots + \beta_n y^{n-1} + \cdots \quad (3.6.15)$$

Here

$$\beta_n = 4^{n-1} B_n / b^{n-1} \quad (3.6.16)$$

and we tabulate the  $\beta_n$ :

$\beta_2$	=	4
$\beta_3$	=	10
$\beta_4$	=	18.364768
$\beta_5$	=	28.224512
$\beta_6$	=	39.81514752
$\beta_7$	=	53.34441984
$\beta_8$	=	68.5375488
$\beta_9$	=	85.8128384
$\beta_{10}$	=	105.775104
$\beta_{11}$	=	128.974848
$\beta_{12}$	=	155.189248

Table 3.2: Reduced virial coefficients for the hard sphere gas

This was the Carnahan and Starling train of argument:

- they observed that the  $\beta_n$  coefficients were “close to” integers;
- they noted that if they rounded to whole numbers: 4, 10, 18, 28, 40, then  $\beta_n$  was given by  $(n-1)(n+2)$ ;
- they then made the assumption that this expression would work for the higher-order terms as well;
- this enabled them to sum the virial series, to obtain an equation of state in closed form.

So they had a suggestion for the values of the virial coefficients to *all* orders. We can check their hypothesis, based upon the coefficients known to them, by comparison with the newly-known virial coefficients.

$n$	2	3	4	5	6	7	8	9	10	11	12
rounded true $\beta_n$	4	10	18	28	40	53	69	86	106	129	155
C+S: $(n-1)(n+2)$	4	10	18	28	40	54	70	88	108	130	154

The agreement is not quite perfect, but it is still rather good.

The Carnahan and Starling virial series is then

$$\begin{aligned}
 \frac{pV}{NkT} &= 1 + 4y + 10y^2 + 18y^3 + 28y^4 + 40y^5 + \dots \\
 &= 1 + \sum_{n=2}^{\infty} (n-1)(n+2)y^{n-1} \\
 &= 1 + \sum_{n=1}^{\infty} n(n+3)y^n.
 \end{aligned}
 \tag{3.6.17}$$

The series is summed, to give

$$\begin{aligned}
 \frac{pV}{NkT} &= 1 + \frac{2y(2-y)}{(1-y)^3} \\
 &= \frac{1+y+y^2-y^3}{(1-y)^3}.
 \end{aligned}
 \tag{3.6.18}$$

This is the Carnahan and Starling equation of state. In Fig. 3.20 we have plotted this equation together with molecular dynamics simulation data from Bannerman *et al.*[16]. The agreement between the Carnahan and Starling

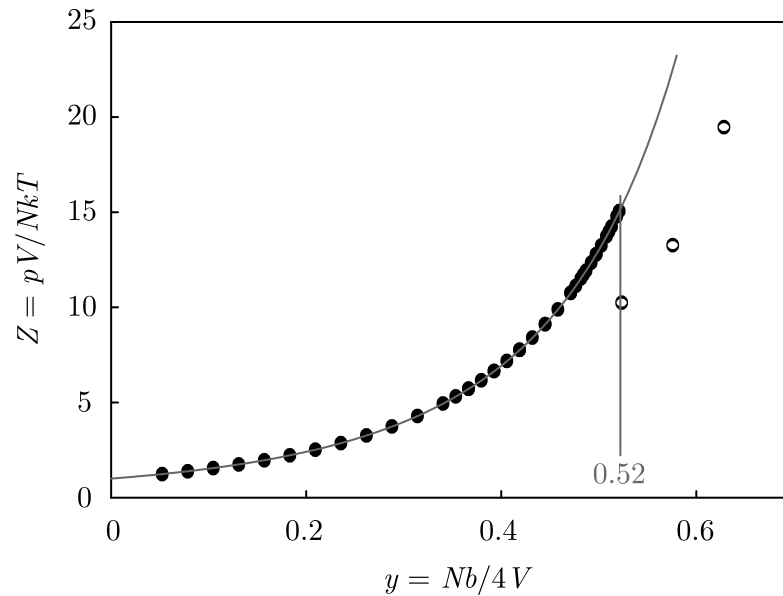


Figure 3.20: Molecular dynamics simulation data plotted with the Carnahan and Starling equation of state

equation of state and the molecular dynamics data is highly impressive. The



drop in  $pV/NkT$  at  $y = 0.524$  is “associated” with the transition to a solid phase.

From Carnahan and Starling’s model the general expression for the  $n$ th virial coefficient is

$$B_n = \frac{(n-1)(n+2)}{4^{n-1}} b^{n-1} \quad (3.6.19)$$

These are listed in Table 3.6.5 together with the true values.

	Calculated	C+S value
$B_2/b$	= 1	1
$B_3/b^2$	= 0.625	0.625
$B_4/b^3$	= 0.28694950	0.28125
$B_5/b^4$	= 0.11025200	0.10937500
$B_6/b^5$	= 0.03888198	0.03906250
$B_7/b^6$	= 0.01302354	0.01318359
$B_8/b^7$	= 0.00418320	0.00427246
$B_9/b^8$	= 0.00130940	0.00134277
$B_{10}/b^9$	= 0.00040350	0.00041199
$B_{11}/b^{10}$	= 0.00012300	0.00012398
$B_{12}/b^{11}$	= 0.00003700	0.00003672

Table 3.3: Carnahan and Starling’s hard sphere virial coefficients

Incidentally, the universal function  $g(n)$  of Eq. (3.6.8) is then given by

$$g(n) = \frac{n^2 b}{2} \frac{(2 - \frac{1}{4}nb)}{(1 - \frac{1}{4}nb)^3}. \quad (3.6.20)$$

A more systematic way at arriving at an equation of state is the Padé method.

### 3.6.6 Padé approximants

The equation of state of the hard sphere gas takes the form

$$\frac{pV}{NkT} = f(y), \quad (3.6.21)$$

where we are writing  $y = Nb/4V$  and  $f$  is a universal function of its argument. So if the function is determined then the hard sphere equation of state is known.

The virial expansion gives  $f$  as a power series in its argument. And in reality one can only know a finite number of these terms. The Carnahan and

Starling procedure took the known terms, it guessed the (infinite number of) higher-order terms and it then summed the series. The figure above indicates that the result is good, but it relied on guesswork and intuition.

For the Carnahan and Starling equation of state the function  $f$  may be written as

$$f(y) = \frac{1 + y + y^2 - y^3}{1 - 3y + 3y^2 - y^3} \quad (3.6.22)$$

In this form we observe that  $f(y)$  is the quotient of two polynomials. And this leads us naturally to the Padé method; this is the general framework for making approximations as such quotients.

One knows  $f(x)$  to a finite number of terms, say  $N$ . The Padé method provides a systematic procedure for approximating the higher-order terms and summing the series. In the Padé method the true function  $f(x)$  is approximated by the quotient of two polynomials

$$f(x) \approx F_{nm}(x) = \frac{P_n(x)}{Q_m(x)}. \quad (3.6.23)$$

Here  $P_n(x)$  and  $Q_m(x)$  are polynomials of degrees  $n$  and  $m$  respectively:

$$\begin{aligned} P_n(x) &= p_0 + p_1x + p_2x^2 + \dots + p_nx^n, \\ Q_m(x) &= q_0 + q_1x + q_2x^2 + \dots + q_mx^m. \end{aligned} \quad (3.6.24)$$

Without loss of generality we may (indeed it is convenient to) restrict  $q_0 = 1$ . This will ensure the coefficients  $p_i, q_j$  (for a given  $n, m$ ) are unique.

All the coefficients of  $P_n(x)$  and  $Q_m(x)$  may be determined so long as  $f(x)$  is known to at least  $n + m$  terms. In other words if  $f(x)$  is known to  $N = n + m$  terms then  $F_{nm}(x)$  agrees with the known terms of the series for  $f(x)$ . However the quotient generates a sequence of higher order terms as well. And the hope is that this series will be a good approximation to the true (but unknown)  $f(x)$ .

The power series of

$$f(x)Q_m(x) - P(x) \quad (3.6.25)$$

begins with the term in  $x^{m+n+1}$ . In other words the coefficient of this and the higher powers are “manufactured” by the Padé procedure.

One can construct approximants with different  $m, n$  subject to  $m+n = N$ . See Reichl[2] for (some) details. Essentially there will be a subset of  $m, n$  pairs whose Padé approximants appear similar, usually when  $m \sim n \sim N/2$ . These “robust” approximants would be expected to provide a good approximation to the true function.

In this way in 1964 Ree and Hoover[18], using the then known  $B_2$  to  $B_6$  (i.e. before Clisby and McCoy's extra virial coefficients) constructed the 3-2 Padé approximant:

$$\frac{pV}{NkT} = \frac{1 + 1.81559y + 2.45153y^2 + 1.27735y^3}{1 - 2.18441y + 1.18916y^2}. \quad (3.6.26)$$

This is plotted as the solid line in Fig. 3.21. For comparison the dotted line shows the truncated virial series up to  $B_6$ .

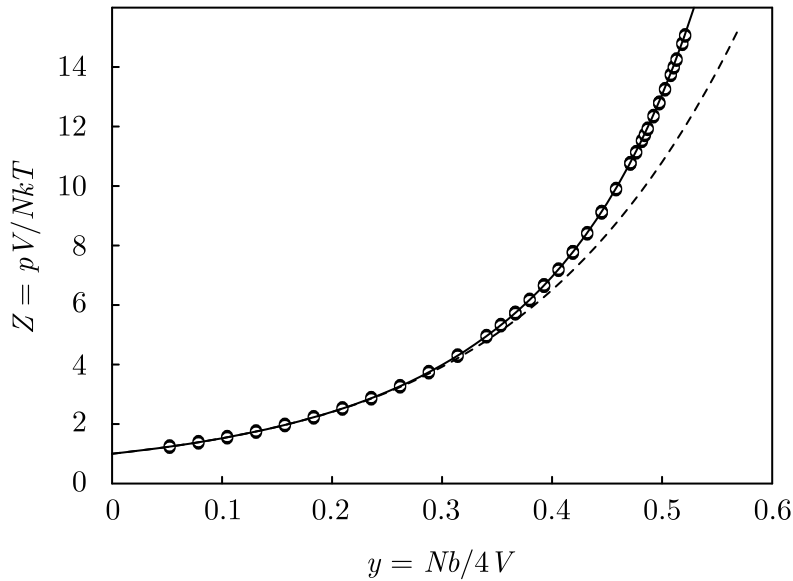


Figure 3.21: The 3-2 Padé approximant (solid line) and truncated virial series up to  $B_6$  (dashed line) shown with molecular dynamics simulations of the hard sphere gas

Observe the 3-2 Padé gives very good agreement with the molecular dynamics data. By contrast the corresponding truncated virial series is essentially useless; this indicates the value of the Padé procedure. We show the original Ree-Hoover results in Fig. 3.22. Note, however, they use a different density scale:  $\frac{V_0}{V} = \frac{\sqrt{18}}{\pi}y$ , moreover they only had *four* molecular dynamics data points and there is no evidence of solidification.

### 3.7 Bridge to the next chapter

The intention of this chapter has been to show how inter-particle interactions change the properties of a gas from the canonical ideal gas behaviour. In-

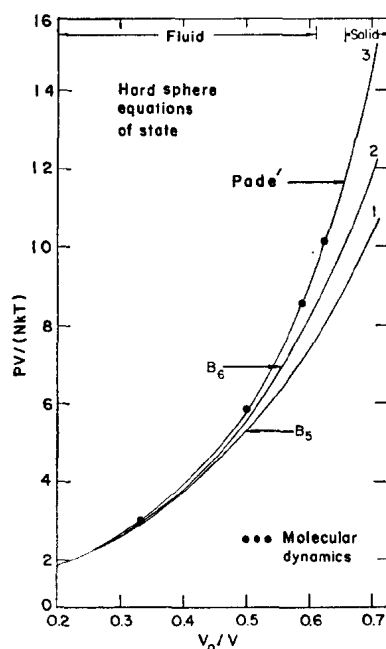


Figure 3.22: Ree and Hoovers Padé approximation to the hard sphere equation of state

interactions were assumed to be “sufficiently weak” so that the behaviour was still gas-like. We know that when interactions are stronger they can result in a qualitatively different phase; thus a gas might condense into a liquid or even into a solid. The next chapter is devoted to the study of phase transitions. It follows logically; this chapter was concerned with the weaker effects of interactions and the next chapter with stronger effects.

There are however, in this chapter, two significant pointers to the next. The major part of the chapter considered the interaction as a small parameter and expansions in powers of this small parameter were obtained. The van der Waals treatment in Section 3.4 was an exception. That had no small parameter and we noted that the resultant equation of state indicated some non-physical behaviour in Fig. 3.19. We shall see that is indicative of a phase transition.

In this context the hard sphere gas also deserves mention. True, this is an expansion in a small parameter – here most sensibly regarded as density. And the knowledge of a (limited) number of the virial coefficients tells us how the resultant behavior of the gas is altered from that of the ideal gas. However in both the Carnahan and Starling procedure and in the Padé approach *all* terms of the virial expansion were approximated/estimated and the infinite

series was summed to give an equation of state in closed form. Then, to the extent that the higher-order coefficients are correct, the summed series should indicate the behaviour at *all* densities up to the radius of convergence.

### 3.7.1 Van der Waals model

The lowest temperature van der Waals isotherm in Fig. 3.19 exhibits unphysical behaviour. We see that for some pressures there are *three* possible volumes. Moreover there is a region of the isotherm where  $\partial p/\partial V$  is *positive*. That is saying that when the pressure is increased the volume increases as well. This is impossible; such a system would be unstable.

These matters will be discussed extensively in the next chapter. However at this stage we simply point out that the calculated equation of state applies fundamentally to a *homogeneous* system. And for certain values of  $p$ ,  $T$  and  $V$  homogeneous state may be unstable, with the corresponding stable state comprising a *coexistence* of phases: a pointer to the next chapter.

### 3.7.2 Hard sphere model

We plot the Bannerman *et al.* molecular dynamics data yet again in Fig. 3.23. This time we plot  $Z = pV/NkT$  on a logarithmic scale in order to include the high density points omitted from the previous plots. We observe that  $Z$  appears to diverge in the vicinity of  $y = 0.741$ . This corresponds to the density of periodic close packing of spheres (hcp or bcc lattice) at  $y = \pi/3\sqrt{2}$ , shown as the line pcg.

The line rcp corresponds to the densest random close packing of spheres, at  $y = 2/\pi \approx 0.638$ ; so this is the greatest density possible for a gas – or an amorphous solid. However it is believed that the maximum possible density of a gas is  $y = 0.495$  and the minimum possible density of a solid is  $y = 0.545$ . In other words, the density range  $0.495 < y < 0.545$  should be a gas-solid coexistence region. The signature would be a constant pressure in this region. The molecular dynamics data do not support this; rather, they indicate a metastable supercooled gas. Presumably the simulations are not run long enough for the equilibrium state to emerge. However the implication is that the metastable state becomes unstable at  $y = 0.522$ .

Now although a *random* assembly of spheres will pack to a density of  $y = 2/\pi \approx 0.638$ , a close-packed lattice (fcc or hcp) will pack more closely, to a density of  $y = \pi/3\sqrt{2} \approx 0.740$ . So it is understandable that there is a pressure drop at the transition from amorphous to regular solid.

Finally we note that the lack of an attractive part of the inter-particle interaction means that there there is no liquid phase in these models; there

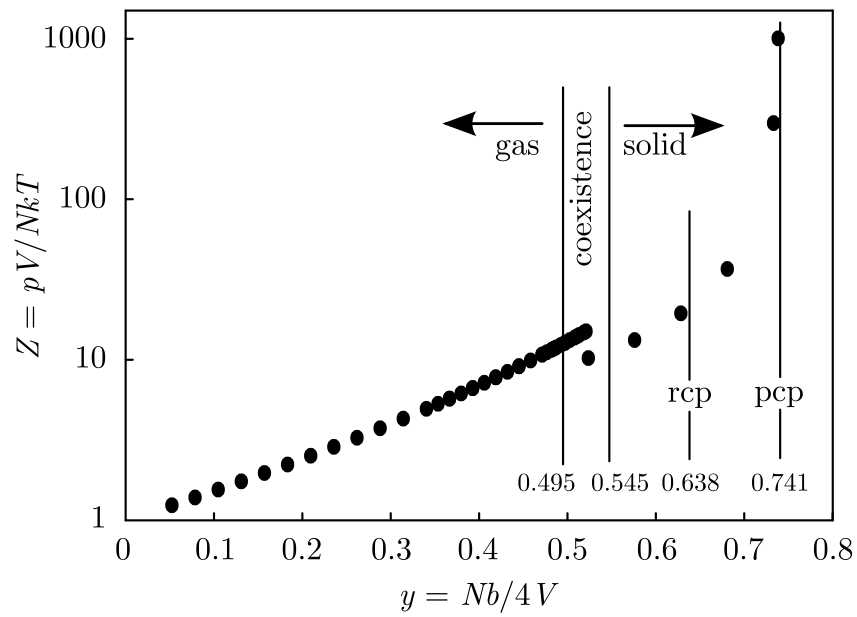


Figure 3.23: Molecular dynamics simulations of the hard sphere equation of state plotted on a logarithmic curve

is no gas-liquid transition. An essential feature of a liquid is that it be *self-bound*. For this there has to be an attractive interaction.

## Further notes

### Microscopic estimation of the van der Waals parameters

#### General form for the $a$ parameter

The van der Waals  $a$  parameter is related to the mean attractive energy per particle  $\langle E \rangle$  by

$$a = \frac{V^2}{N} \frac{d\langle E \rangle}{dV}, \quad (3.7.1)$$

where

$$\langle E \rangle = \frac{1}{2} \frac{N}{V} \int 4\pi r^2 U(r) dr \quad (3.7.2)$$

(from Eqs. (3.4.11) and (3.4.12)). Since the volume dependence is all in the  $1/V$  prefactor, we obtain

$$a = -2\pi \int r^2 U(r) dr. \quad (3.7.3)$$

For any two-parameter interaction energy function, with a scaling energy  $\varepsilon$  and a scaling distance  $\sigma$  we have

$$U(r) = \varepsilon u(r/\sigma), \quad (3.7.4)$$

so that, by changing the variable of integration to  $x = r/\sigma$ ,

$$a = -\varepsilon\sigma^3 \times 2\pi \int x^2 u(x) dx. \quad (3.7.5)$$

The integral here is a dimensionless number, so we obtain the general result

$$a = \varepsilon\sigma^3 \times \text{const.} \quad (3.7.6)$$

We conclude that the van der Waals  $a$  parameter will be given by  $\varepsilon\sigma^3$  multiplied by a model-dependent numerical factor.

#### Model-dependent prefactors

In Fig. 3.24 we show the Lennard-Jones 6 – 12 potential together with the Sutherland potential. The Lennard-Jones potential has the familiar form, as in Eq. (3.2.17)

$$U_{\text{LJ}}(r) = 4\varepsilon \left\{ \left( \frac{\sigma}{r} \right)^{12} - \left( \frac{\sigma}{r} \right)^6 \right\}.$$

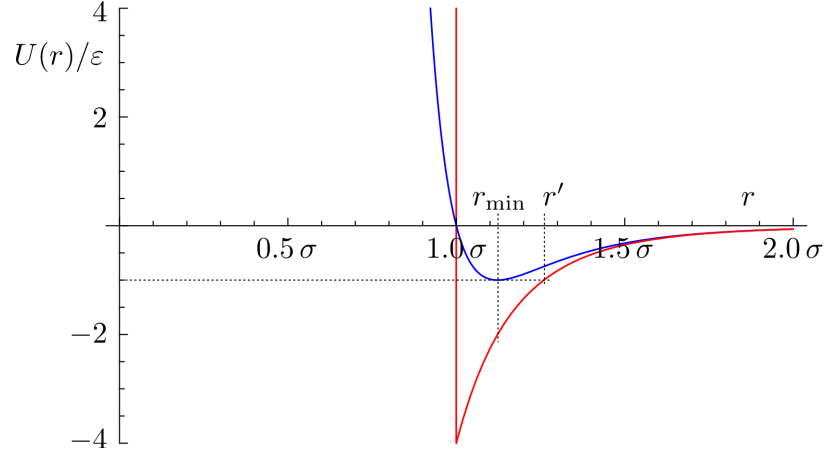


Figure 3.24: Lennard-Jones (blue) and Sutherland (red) potentials. The Sutherland potential has been scaled to that it coincides with the Lennard-Jones potential at large distances.

However we now write the Sutherland potential in a form slightly different to that in Eq. (3.2.25); here we express it as

$$\begin{aligned} U_S(r) &= \infty & r < \sigma \\ &= -4\varepsilon \left(\frac{\sigma}{r}\right)^6 & r > \sigma. \end{aligned} \quad (3.7.7)$$

The factor of 4 here ensures that the Sutherland and the Lennard-Jones potentials coincide at large distances.

Recall that the van der Waals  $\sigma$  parameter represents the effects of the weak attractive part of the inter-particle interaction. So the range of the integral in Eq. (3.7.5) might extend from  $r = \sigma$  up to infinity. In this case

$$a = \frac{16\pi}{9} \varepsilon \sigma^3 = 5.59 \times \varepsilon \sigma^3. \quad (3.7.8)$$

Alternatively, we might go only from the minimum in the Lennard-Jones potential, at  $r = r_{\min} = 2^{1/6}\sigma$ , up to infinity. In that case

$$a = \frac{10\sqrt{2}\pi}{9} \varepsilon \sigma^3 = 4.94 \times \varepsilon \sigma^3. \quad (3.7.9)$$

Since we are considering only the attractive part of the interaction it might be more appropriate to consider the Sutherland potential. Integrating the Sutherland potential (in its Eq. (3.7.7) form) over the entire range  $\sigma \leq r < \infty$  gives

$$a = \frac{8\pi}{3} \varepsilon \sigma^3 = 8.38 \times \varepsilon \sigma^3. \quad (3.7.10)$$



This is clearly a serious over-estimate as the integral incorporates short distances where the attractive potential falls well below the Lennard-Jones minimum of  $-\varepsilon$ ; it falls to  $-4\varepsilon$ . We could remedy this by integrating only from  $r_{\min} = 2^{1/6}\sigma$ , which gives

$$a = \frac{4\sqrt{2}\pi}{3}\varepsilon\sigma^3 = 5.92 \times \varepsilon\sigma^3. \quad (3.7.11)$$

But this is still an overestimate and we might be inclined to integrate from  $r' = 2^{1/3}\sigma$ , where the Sutherland potential has the Lennard-Jones minimum of  $-\varepsilon$ . In that case

$$a = \frac{4\pi}{3}\varepsilon\sigma^3 = 4.19 \times \varepsilon\sigma^3. \quad (3.7.12)$$

A different approach would be to look at the behaviour of the second virial coefficient. The van der Waals equation of state leads to  $B_2$  as given by Eq. (3.4.17):

$$B_2^{\text{VW}}(T) = b - \frac{a}{kT}.$$

By comparison, the attractive tail of the Lennard-Jones potential, as represented by the similar tail of the Sutherland Potential Eq. (3.7.7) will give a second virial coefficient, at high temperatures, of

$$B_2(T) = \frac{2}{3}\pi\sigma^3 \left(1 - \frac{4\varepsilon}{kT}\right). \quad (3.7.13)$$

Consistency of these two equations is ensured through the identification

$$a = \frac{8\pi}{3}\varepsilon\sigma^3 = 8.38 \times \varepsilon\sigma^3. \quad (3.7.14)$$

And we note that this corresponds precisely to the value obtained from integrating the Sutherland potential directly over the range  $\sigma \leq r < \infty$ , Eq. (3.7.10).

### 3.7.3 Other bit – Tabulation of - - - -

Some values from Duda [22].

	$kT_c/\varepsilon$	$kT_B/\varepsilon$	$kT_i/\varepsilon$	$z_c$	a
Square Well ( $R = 1.65$ )	a	a	a	a	a
Lennard-Jones	1.326	3.418	6.431	0.281	a
Sutherland	0.595	1.171	2.252	0.303	a